

An Approach to Identify Urban Waterlogging on a Deltaic Plain using ArcGIS on CHD based Flow Accumulation Models

Kaushik Bhaumik

Jadavpur University

Subhasish Das (✉ subhasishju@gmail.com)

Jadavpur University <https://orcid.org/0000-0002-6512-7454>

Research Article

Keywords: Run-off, flow accumulation, waterlogging, gradient, aspect

Posted Date: June 10th, 2021

DOI: <https://doi.org/10.21203/rs.3.rs-230413/v1>

License:  This work is licensed under a Creative Commons Attribution 4.0 International License.

[Read Full License](#)

An Approach to Identify Urban Waterlogging on a Deltaic Plain using ArcGIS on CHD based Flow Accumulation Models

Kaushik Bhaumik^a and Subhasish Das^{a,*}

^aSchool of Water Resources Engineering, Jadavpur University, Kolkata, West Bengal, India

*Corresponding Author. *Email address*: subhasish.das@jadavpuruniversity.in

ABSTRACT

The gradient for any point on the land surface can be calculated using the digital-elevation model. Some empirical correlations are available to determine the gradient of any points. A few studies were conducted for hilly forest areas to determine the aspect and gradient of various points using computational hydrodynamics (CHD) based techniques. On a plain surface, the accuracy of such techniques was rarely verified. The application of such techniques for a plain surface is also extremely challenging for its small slope. Therefore, the prime objective of the present study is to find out an advanced technique to more accurately determine the gradient of various points on a plain surface which may help in determining the key areas affected by run-off, subsequent flow accumulation, and waterlogging. Here, Kolkata city as a deltaic plain surface is chosen for this study. Upto 600 m × 600 grid sizes are used on the DEM map to calculate the run-off pattern using a D8 algorithm method and second-order, third-order, and fourth-order finite difference techniques of CHD. After finding out the gradient, the run-off pattern is determined from relatively higher to lower gradient points. Based on the run-off pattern, waterlogging points of a plain surface are precisely determined. The results obtained from all the different methods are compared with one other as well as with the actual waterlogging map of Kolkata. It is found that the D8 algorithm and fourth-order finite-difference-technique are the most accurate while determining the waterlogging areas of a plain surface. Next, true gradients of waterlogging points are calculated manually to compare the calculated gradient points using each method. This is also done to determine the relationship and error between the true and calculated gradient of waterlogged points using various statistical analysis methods. The relationship between true and calculated gradients is observed from weak to strong if the D8 algorithm is replaced by the newly introduced fourth-order finite difference technique. Better accuracy and stronger relationships can be achieved by using a smaller grid size.

Keywords: Run-off; flow accumulation; waterlogging; gradient; aspect.

1. Introduction

Urban migration and agriculture can be considered as major causes of landscape change in numerous parts of the earth (Vizzari et al., 2018). With the increase in population, cities around the world are adopting flood water management measures to trim down the damage to the environment caused by impermeable run-off (Grey et al.

44 2018). It is, therefore, necessary to determine the flow accumulation and thereby the water-
45 logging points in order to design a drainage system in the most effective way. Different
46 techniques are used for evaluating the overall performance of the estimation, its accuracy and
47 precision, and the self-reliance of estimation inaccuracy, as well as the magnitude of the
48 slopes measured in the field (Warren et al. 2004).

49 Recently the digital-elevation-models or DEMs are used as input information for
50 determining the flow directions in hydrological models for discharge simulation due to their
51 high efficiency in presenting the spatial variability of the earth's surface (Beven and Kirkby
52 1979; Beasley et al. 1980; Fortin et al. 2001). The DEM accuracy was verified for different
53 terrain parameters (Guo-an et al. 2001). Numerous grid DEM-based algorithms are also used
54 and implemented in many GIS software programs for various hydrological analyses
55 (O'Callaghan and Mark 1984; Fairfield and Leymarie 1991; Quinn et al. 1991; Bolstad and
56 Stowe 1994; Cabral and Burges 1994; Tarboton 1997; Ashraf et al. 2011). Some empirical
57 formulas are also used for determining the flow direction. Xue et al. (2016) used numerical
58 simulation for determining the waterlogging area of an urban area.

59 Skidmore (1989) used six different methods to find out aspect and slope (gradient) from
60 a commonly gridded DEM in a geographical region in southeast Australia having moderate
61 topography. However, a definite study using the computational hydrodynamics (CHD)
62 method to find out the slope on a plain surface was rarely done earlier.

63 The most widely used method to determine the run-off pattern in a surface is the D8
64 method described by Martz and Garbrecht (1992), The method was termed the deterministic
65 eight neighbors (D8) technique by Fairfield and Leymarie (1991). Based on the fact that the
66 water in every DEM grid-cell flows to only one of the neighboring cells, heading for a much
67 larger drop. Some researchers (Zhao et al. 2009) used empirical formulas to determine the
68 flow pattern.

69 Skidmore (1989) earlier used this method for a hilly forest area over a 100 square km
70 area of southeast Australia. He used the following methods for calculating the gradient
71 (slope) and the aspect of various points.

- 72 1 Conventional D8 algorithm (D8A)
- 73 2 Similar to the D8A method with the highest slope with the steepest fall or mount
- 74 3 Finite difference method of second order (FD2O)
- 75 4 Finite difference technique of third order (FD4O)
- 76 5 two methods using multi linear model using regression

77 These five types of methods were quantitatively compared by taking three consecutive
78 horizontal and three consecutive vertical grid cells. The differences between the true aspect
79 and the estimated aspect calculated using six methods as mentioned above were also
80 calculated. The basic purpose of the study was to visualize these methods, which have a
81 much smaller deviation than the true values of the slope and aspect. Skidmore (1989)
82 concluded that there was almost no difference between third order method and multi
83 regression models for calculating slope (gradient) and aspect. Between these methods, the
84 FD3O method i.e. the finite difference technique of third order was found to be most
85 accurate.

86 It is noteworthy to mention that using computational hydrodynamics to solve the partial
87 differential equation and thereby determining the run-off pattern in a plain surface was hardly

88 ever done earlier. The challenge to determine the flow accumulation and waterlogging
89 areas on a plain surface is more than a semi-hilly or hilly surface because of the much
90 smaller deviation of the elevations in between the consecutive grids. Here it is intended
91 to find the usability of the following methods to determine the potential flow
92 accumulation areas thereby the waterlogging areas on a plain surface. Like Skidmore,
93 here first three methods are evaluated for a plain surface.

- 94 ○ Conventional D8 algorithm (D8A)
- 95 ○ Finite difference technique of second order (FD2O)
- 96 ○ Finite difference technique of third order (FD3O)
- 97 ○ Finite difference technique of fourth order (FD4O)

98 The fourth-order finite-difference technique (FD4O) is a new method, which was
99 not used by Skidmore (1989) or others. The basic purpose of introducing this method is
100 to check whether a more accurate result can be obtained than the second or third-order
101 finite-difference technique.

102 Skidmore (1989) found the FD3O method to be the most accurate only for hilly
103 forest areas. From the literature reviews, it is clear that till now any accurate technique
104 was neither proposed nor verified to identify the waterlogging areas on a plain surface.

105 To find out the waterlogging area, one needs to first calculate the gradient values.
106 After finding the waterlogging area of a plain surface, calculated gradient values have
107 been compared for a few points (waterlogged area) with true values and thereby
108 determined the Spearman rank coefficient to find out the relationship between these two
109 variables. Based on the observations on area matching accuracy and better Spearman
110 correlation values, the most appropriate method for determining flow accumulated and
111 waterlogged areas have been recommended.

112 So, in conclusion, the prime objective of this study is to use four different methods
113 D8A, FD2O, FD3O, and FD4O to find out the waterlogging area on a plain surface to
114 develop further stormwater networks and related pumping systems. It is also important to
115 find out which method is more accurate on a plain surface. Out of these four methods, it
116 is also found out which method is the most suitable for a plain surface.

117

118 2. Study area volition

119

120 For the study area, the deltaic city Kolkata is chosen as a plain surface. The deltaic
121 city Kolkata is the capital of West Bengal state in India as shown in Fig. 1. The megacity
122 is situated on the lower Ganga-Bhagirathi Rivers plain, and the River Hooghly (a
123 tributary of River Ganga) extends its western boundary from 22⁰28' north to 22⁰37'30"
124 north and 88⁰17'30" east to 88⁰25' east covering around 187 sq. km area. This metro city
125 is divided into 144 wards (including the addition of three more wards recently). Most of
126 the plains are covered by the Hooghly River to the northwest and numerous canals such
127 as Bagjola in the north, Belighata, and the central circular canal, and the Adi-Ganga and
128 Tolly Nallah in the southern part, but most of these rivers and nalas have been silted up
129 (John and Das 2020). The plain area of Kolkata is largely divided into nine numbers of
130 drainage basins. Among these nine basins, three of them cater to western Kolkata and the
131 remaining six of them serve the eastern portion. Total eleven numbers of sluice ways

132 connecting the river Hooghly prevent the entry of many tidal waves during the worst events.
133 This deltaic plain land is located at an average elevation of 9.1 meters above sea level, tilted
134 to the south. The metropolis has several low-lying areas such as shallow waterbodies with
135 marshes, many of which are remnants of the Bhagirathi river waterways. Megacity Kolkata is
136 bounded north and east by the 24 Parganas (N) and in the south by the 24 Parganas (S) and
137 the Howrah to the west. The area encounters a tropical climate with the highest temperature
138 of approx. 40°C and with a minimum temperature of about 10°C, corresponding to a moderate
139 rainfall of 165cm where 70-80% of annual rainfall takes place between mid June to early
140 September (John and Das 2020). The population of Kolkata based on the 2011 census was
141 4,496,694 and the metropolitan population had 14,112,536 people in 2011. Mukhopadhyay
142 (2004) and Paul (2009) reported an overall situation of terrible waterlogging problems in
143 Kolkata city.

144 Though waterlogging has been a foremost trouble in all monsoons in Kolkata but large
145 this plain area has evidenced a series of severe floods in the succeeding years of 1970, 1978,
146 1984, 1999, 2007, 2016 flooding densely or moderately populated plain areas in the central
147 part of the city like Central Avenue, Bidhan Sarani, Sealdah, Amherst Street, Park Circus
148 Connector, Bowbazar, Park Street, Suryasen Street and its connected areas and in the
149 southern Kolkata including Jadavpur, Behala, Deshapriya Park. Gariahat (Dasgupta et al.
150 2012).

151 The cause of waterlogging nature in Kolkata is divided into the following categories
152 (Banerjee 2018).

- 153 ○ Topography: A low-lying city on the shore of River Hooghly (average elevation of
154 9.1 meters above sea level) on the west and a wetland towards the east, several natural
155 depressions, a layer of active clay. The city's natural gradient extends from west to
156 east, with Hooghly outlining the western boundary. The central area of Kolkata city is
157 like a bowl of soup with stormwater coming in from the neighbouring areas.
158 Previously, the eastern part included wetlands and large swamps where stormwater
159 could enter and were the natural sinks of the city's sewage system.
160
- 161 ○ Governance Issue: The Kolkata drainage system is perhaps the oldest one - probably
162 no improvement after that has forced the city into a poorer condition. The high levels
163 of siltation, inadequate and improper sewer arrangements, unscientific canals (nalas)
164 are the main issues. Heavy siltation has greatly decreased the transport capacity of
165 River Hooghly. Dredging is predominantly perfunctory and yet, it is not possible to
166 divert the city's stormwater by pumping into the Hooghly River during the high tides.
167 Given all these issues that are the reason for waterlogging, it is certain that the people
168 of Kolkata have to stop living underwater every few hours of heavy rain.
169
- 170 ○ Anthropogenic Issue: Increase in population density, urbanisation and a huge amount
171 of concretization, reduction in greenery and water body, lack of awareness of
172 abundance have led to urban flood problems.
173
- 174 ○ Climatic Condition: Climate change is one of the reasons for urban flooding.

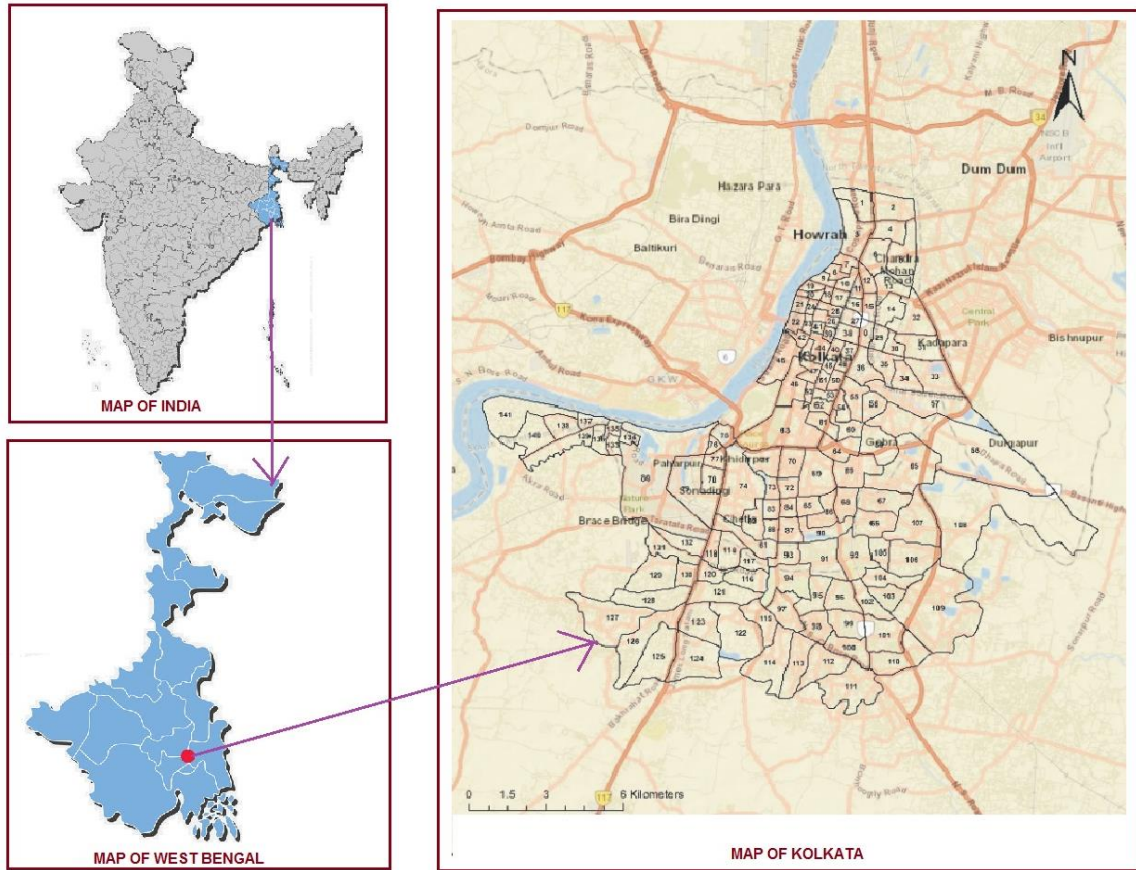


Fig. 1. Study area

3. Research methodology

In this study, we have used the DEM of Kolkata city as a plain surface. The ultimate goal of this study is to identify the most accurate method for finding out the waterlogging areas of a plain area like Kolkata. The DEM grid contains the structure of the matrix data and each matrix node stores the geographic elevation of every pixel. DEMs are readily available and easy to use which is why they have seen widespread use in the various analyses of hydrologic problems (Moore et al., 1991). The methods describe various means of calculating the slope of each grid point of DEM point and then calculating run-off and waterlogging patterns.

3.1. D8 algorithm technique (D8A)

In this method, the gradient is calculated as the path to the highest drop from the centre cell to the nearest eight cells as given in Fig. 2 wherein the central point elevation magnitude of the 9×9 matrix is denoted as $z_{i,j,k}$ such that i, j and k symbolize the directional nodes along with horizontal (x), crosswise (y) and elevation wise (z) directions, respectively. The corresponding gradient calculation formula is given in equation 1.

The formula is,

$$\text{Gradient} = \max \left[\left\{ z_{i,j,k} - z_{i-1,j-1,k} \right\}, \left\{ z_{i,j} - z_{i-1,j,k} \right\}, \dots, \left\{ z_{i,j,k} - z_{i+1,j+1,k} \right\} \right] \quad (1)$$

$Z_{i-1,j+1,k}$	$Z_{i,j+1,k}$	$Z_{i+1,j+1,k}$
$Z_{i-1,j,k}$	$Z_{i,j,k}$	$Z_{i+1,j,k}$
$Z_{i-1,j-1,k}$	$Z_{i,j-1,k}$	$Z_{i+1,j-1,k}$

Fig. 2. A 9×9 cell matrix.

199

200

201

202 For the terminal grid points of the DEM map; the nearest point outside the DEM of
 203 Kolkata has been considered for calculation purposes. Using this method gradient is
 204 calculated for all the points of the DEM. The run-off pattern is calculated by comparing the
 205 difference in the gradient of any value and eight nearest cells. The maximum difference
 206 between any of these two points is to the direction of run-off and accordingly, the run-off
 207 pattern is calculated for all the points.

208

209 3.2. Finite difference technique of second order (FD2O)

210

211 Our second method deals with finite difference of second order (FD2O) model by which the
 212 gradient is calculated. The first step is to calculate $(\delta z/\delta x)_{i,j,k}$, and $(\delta z/\delta y)_{i,j,k}$ using the second-
 213 order finite- difference technique. Equations 2-3 are explained below.

214

$$\left[\frac{\delta z}{\delta x} \right]_{i,j,k} \approx \frac{z_{i+1,j,k} - z_{i-1,j,k}}{2\Delta x} \quad (2)$$

215

$$\left[\frac{\delta z}{\delta y} \right]_{i,j,k} \approx \frac{z_{i,j+1,k} - z_{i,j-1,k}}{2\Delta y} \quad (3)$$

216 Here Δx is the smallest spacing between grid positions in the plain (x) direction, spacing
 217 Δy is the smallest distance between the grid points in the crosswise (y) path, and i and j
 218 indices are must not the side-line columns or rows. Here, k is the elevation (z) wise index.

219 For the points at the end of a row of columns, equations 4-5 obtained using a polynomial
 220 technique with the second-order difference (Anderson 1995), have been used to calculate
 221 gradient components.

$$\left[\frac{\delta z}{\delta x} \right]_{i=n,j,k} \approx \frac{-3z_{i=n,j,k} + 4z_{i=n+1,j,k} - z_{i=n+2,j,k}}{2\Delta x} \quad \text{where } n = 1,2,3,\dots \quad (4)$$

$$\left[\frac{\delta z}{\delta y} \right]_{i,j=n,k} \approx \frac{-3z_{i,j=n,k} + 4z_{i,j=n+1,k} - z_{i,j=n+2,k}}{2\Delta y} \quad \text{where } n = 1,2,3,\dots \quad (5)$$

224

The gradient ($\tan G$) is then defined as

$$\tan G = \sqrt{\left[\frac{\delta z}{\delta x}\right]^2 + \left[\frac{\delta z}{\delta y}\right]^2} \quad (6)$$

Again similar to the [D8A method](#), the gradient is calculated for all the points in a grid. The run-off pattern is calculated by comparing the difference in the gradient of any value and eight nearest cells. The maximum difference between any of these two points is the direction of run-off and thus it is calculated for all the points.

230

231 **3.3. Finite difference technique of third order (FD3O)**

232

233 The next method is the finite difference of third order ([FD3O](#)) technique by which the
234 gradient is calculated. Again, $(\delta z/\delta x)_{i,j,k}$ and $(\delta z/\delta y)_{i,j,k}$ are calculated by using the following
235 equations.

$$\left[\frac{\delta z}{\delta x}\right]_{i,j,k} \approx \frac{z_{i+1,j+1,k} - z_{i-1,j+1,k} + 2(z_{i+1,j,k} - z_{i-1,j,k}) + z_{i+1,j-1,k} - z_{i-1,j-1,k}}{8\Delta x} \quad (7)$$

$$\left[\frac{\delta z}{\delta y}\right]_{i,j,k} \approx \frac{z_{i+1,j+1,k} - z_{i+1,j-1,k} + 2(z_{i,j+1,k} - z_{i,j-1,k}) + z_{i-1,j+1,k} - z_{i-1,j-1,k}}{8\Delta y} \quad (8)$$

238 For the points at the end of a row of columns, equations 9-10 obtained using the
239 polynomial technique with the third-order difference, have been used to calculate
240 gradient components.

$$\left[\frac{\delta z}{\delta x}\right]_{i=n,j,k} \approx \frac{-11z_{i=n,j,k} + 18z_{i=n+1,j,k} - 9z_{i=n+2,j,k} + 2z_{i=n+3,j,k}}{6\Delta x} \quad \text{where } n = 1,2,3,\dots \quad (9)$$

$$\left[\frac{\delta z}{\delta y}\right]_{i,j=n,k} \approx \frac{-11z_{i,j=n,k} + 18z_{i,j=n+1,k} - 9z_{i,j=n+2,k} + 2z_{i,j=n+3,k}}{6\Delta y} \quad \text{where } n = 1,2,3,\dots \quad (10)$$

243 The gradient is calculated using equation 6 as described before. Again, similar to
244 the [D8A method](#), gradient $\tan G$ is calculated for all the points in the zone.

245

246 **3.4. Finite difference technique of fourth order (FD4O)**

247

248 The next method is the finite difference of fourth order ([FD4O](#)) technique by which the
249 gradient is calculated. The first step is to calculate $(\delta z/\delta x)_{i,j,k}$ and $(\delta z/\delta y)_{i,j,k}$ which are
250 calculated by the following equations 11-12 derived using CHD and Taylor series technique.

$$\left[\frac{\delta z}{\delta x}\right]_{i,j,k} \approx \frac{-z_{i+2,j,k} + 8z_{i+1,j,k} - 8z_{i-1,j,k} + z_{i-2,j,k}}{12\Delta x} \quad (11)$$

$$\left[\frac{\delta z}{\delta y}\right]_{i,j,k} \approx \frac{-z_{i,j+2,k} + 8z_{i,j+1,k} - 8z_{i,j-1,k} + z_{i,j-2,k}}{12\Delta y} \quad (12)$$

253 For the points at the end of a row of columns, equations 13-14 obtained using the
254 polynomial technique with the fourth-order difference, have been used to calculate
255 gradient components.

$$\left[\frac{\delta z}{\delta x}\right]_{i=n,j,k} = \frac{-25z_{i=n,j,k} + 48z_{i=n+1,j,k} - 36z_{i=n+2,j,k} + 16z_{i=n+3,j,k} - 3z_{i=n+4,j,k}}{12\Delta x} \quad \text{where } n = 1,2,3,\dots \quad (13)$$

257
$$\left[\frac{\delta z}{\delta y} \right]_{i,j=n,k} = \frac{-25z_{i,j=n,k} + 48z_{i,j=n+1,k} - 36z_{i,j=n+2,k} + 16z_{i,j=n+3,k} - 3z_{i,j=n+4,k}}{12\Delta y} \quad \text{where } n = 1,2,3,\dots \quad (14)$$

258 The gradient and run-off pattern are again calculated as described above.

259

260 **4. Results and Discussion**

261

262 As per the research methodology described in the earlier section, first, we need to determine
 263 the elevation value. Raster file was extracted from United-States-Geological-Survey Earth
 264 Explorer. To extract the elevation value from the ASTER Global DEM of Kolkata, ArcGIS
 265 v10.3 software was used. A spatial resolution of 28.58×30.76 m was used. Initially, a 1200 m
 266 × 1200 m grid is used to determine the elevation points of Kolkata covering almost 22800 m
 267 × 19200 m plain surface. In the following picture, the DEM of Kolkata divided into a 1200 m
 268 × 1200 m grid is shown in Fig. 3. The major areas of Kolkata are also shown in this Fig. 3.

269



270 **Fig. 3.** DEM map of Kolkata using a 1200 m × 1200 m grid.

271

272
 273 The elevation data of various points of Kolkata is extracted from the software FishNET
 274 is indicated below. Using the elevation data from Fig. 4, the gradient is calculated using the
 275 **D8A and FD20 methods.**

276 **In the D8A method,** initially, the 1200 m × 1200 m grid has been used. This is explained
 277 using equation 1. In Fig. 4, the elevation data of Kolkata has been extracted from DEM. All
 278 the elevation values indicated here are respecting the mean-sea-level. The cells as highlighted
 279 in Fig. 4 are used for showing sample calculation to determine the gradient value of a point.
 280 The elevation value of the center cell is highlighted in yellow ($z_{i,j,k}$) is 14. Differences from
 281 the adjacent cells are calculated below.

282

283 **Sample Case 1:**

$$14-08=6 \qquad 14-05=9$$

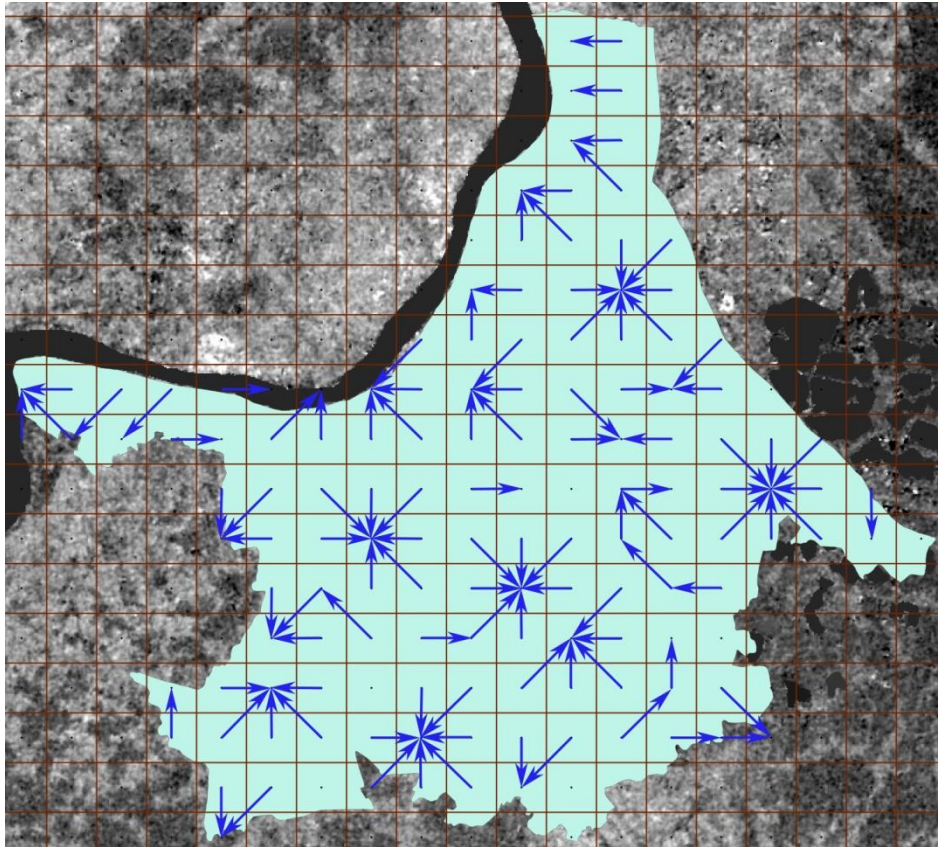


Fig. 6. Runoff pattern using the D8A method.

303

304

305

306 The **FD20 method** elucidates the second-order finite-difference technique. Here $1200\text{ m} \times$
 307 1200 m grid has been used. The elevation data of Kolkata is already indicated in Fig. 4. Using
 308 equations 2-5, $(\delta z/\delta x)_{i,j,k}$ and $(\delta z/\delta y)_{i,j,k}$ values are calculated. Using the values $(\delta z/\delta x)_{i,j,k}$, and
 309 $(\delta z/\delta y)_{i,j,k}$ gradient of all elevation points have been calculated using equation 6. The run-off
 310 pattern has been calculated similarly to the **D8A method** and shown below in Fig. 7.

311

312 From the analysis of the above two (2) methods i.e. **D8A and FD20 methods**,

313 it is found that the gradient of the respective points is not matching each other.

314 Therefore, the run-off pattern and waterlogging area of Kolkata cannot be determined

315 more accurately using a $1200\text{ m} \times 1200\text{ m}$ grid. Since the area of Kolkata is not much,

316 a better result is expected to be obtained if we use more closely spaced grids such as

317 $800\text{ m} \times 800\text{ m}$ grid or even smaller like $600\text{ m} \times 600\text{ m}$ grid.

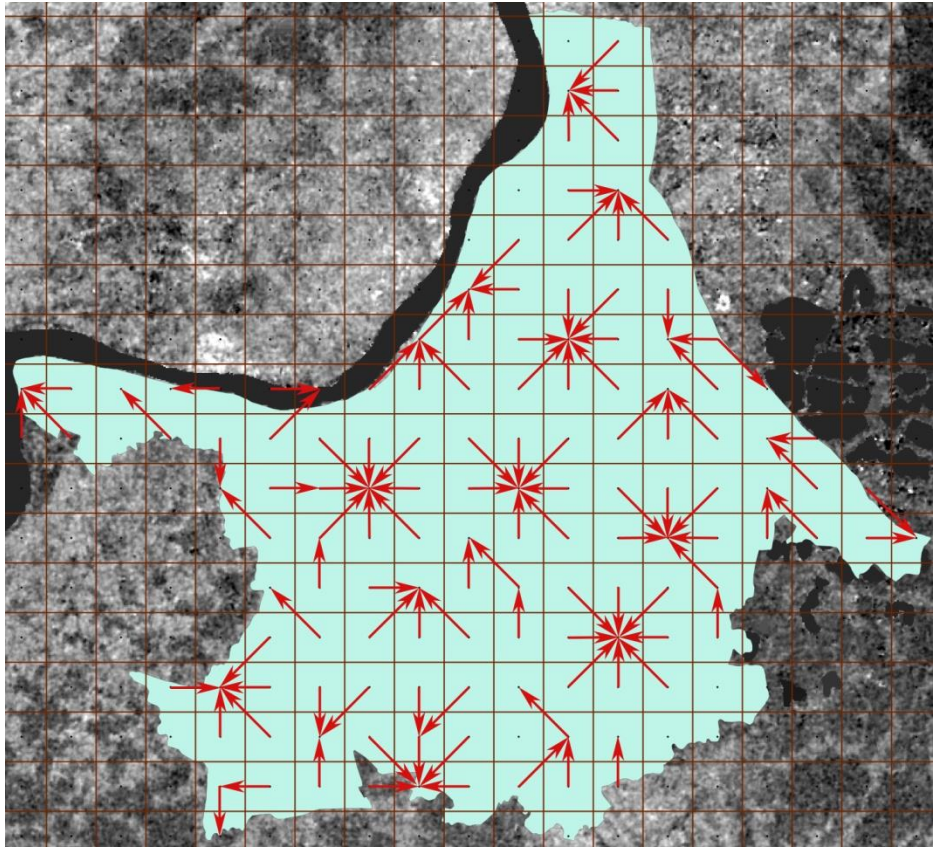


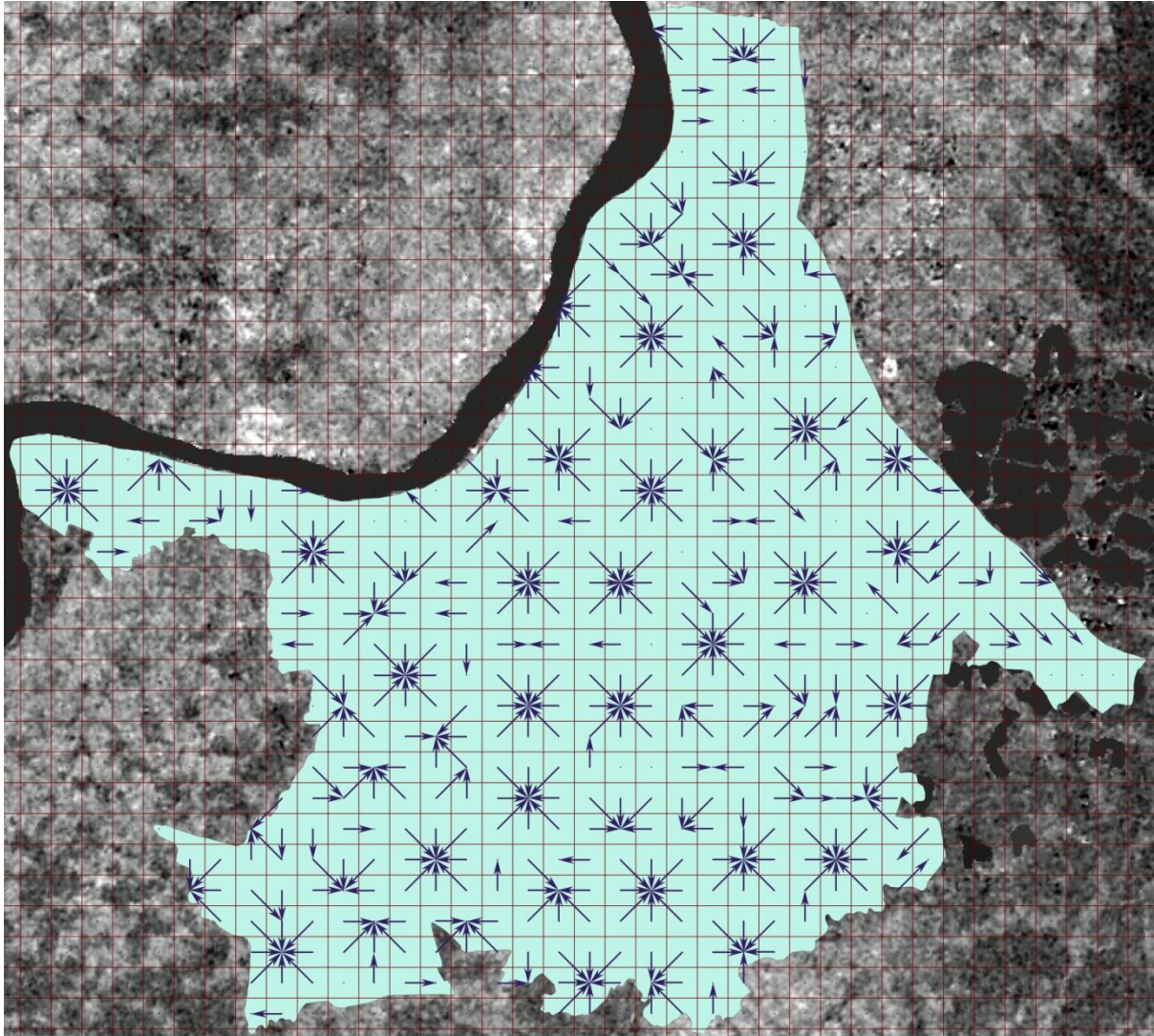
Fig. 7. Runoff pattern using the FD2O method.

318
 319
 320
 321
 322
 323
 324
 325
 326
 327
 328
 329
 330
 331
 332

Therefore, for better accuracy using the purpose using the FishNET tool of ArcGIS software, the entire DEM of Kolkata is divided into a 600 m × 600 m grid as indicated in Fig. 8 below. The gradient of all the points and runoff patterns is calculated using the two methods explained above and also using the third and fourth-order differential methods (FD3O and FD4O). Later using all these methods waterlogging area of Kolkata is determined. Hence, we restrict the grid size with a 600 m × 600 m grid and different calculations are done to calculate the gradient and thereby flow pattern and waterlogging area of Kolkata.

Elevation data extracted from the DEM using ArcGIS is indicated in Fig. 9. The gradient of the various points is then calculated of the above points and thus run-off pattern and potential waterlogging area of Kolkata is determined using all four (4) methods.

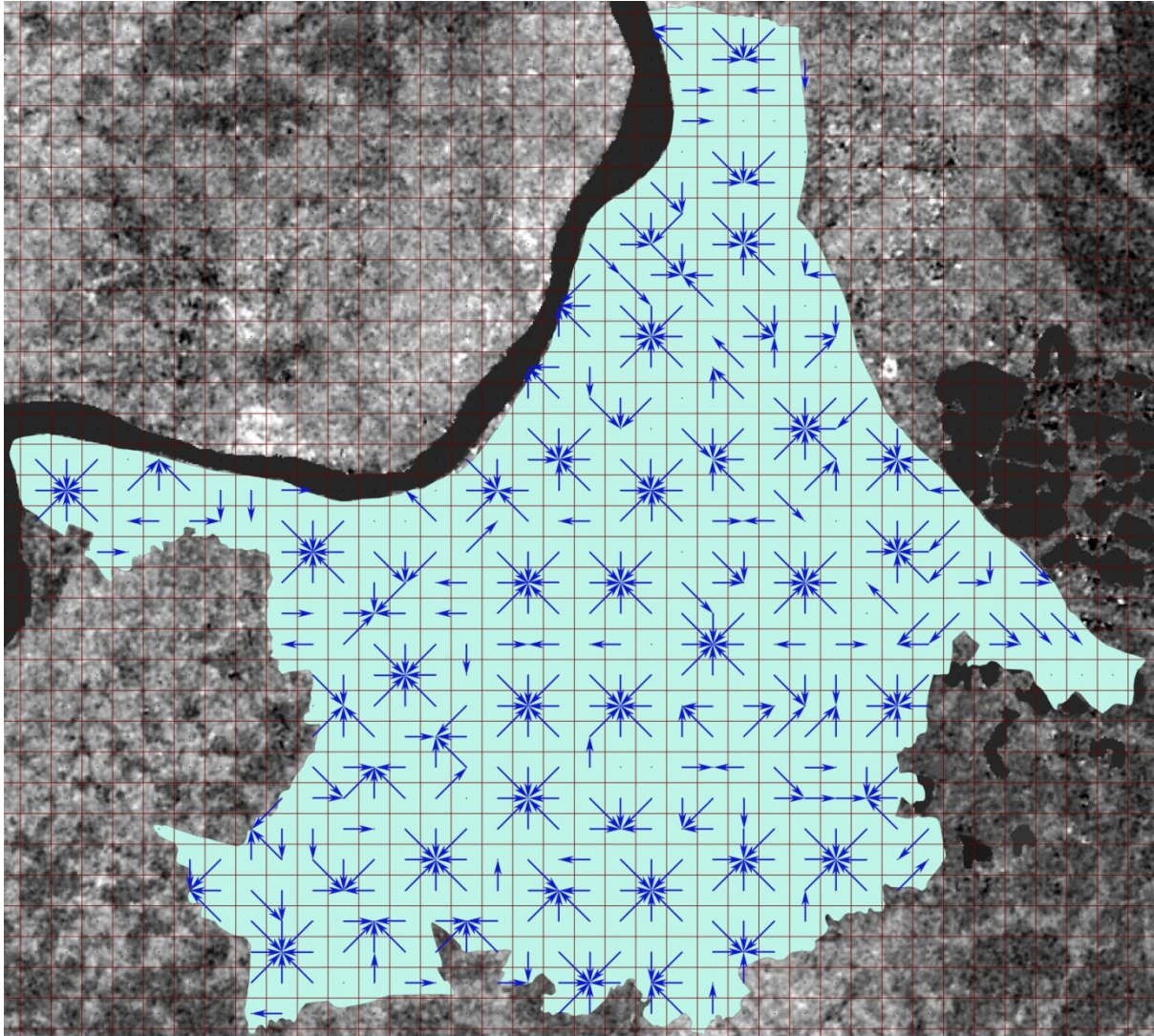
340 Elevation data of Kolkata in $600\text{ m} \times 600\text{ m}$ grid is tabulated in Fig. 9. Similar to the
341 earlier method integer values are only considered for the elevation of different points. Here,
342 we have used the **D8A** method to determine the flow pattern. This method is explained in
343 equation 1. First, the gradient, $\tan G$ is calculated for all elevation points. The run-off pattern
344 is then calculated by comparing the difference of gradient of any point and the next eight
345 nearest cells and shown in Fig. 10.
346



347
348 **Fig. 10.** Run-off pattern using **D8A** method.
349

350
351
352
353
354
355
356
357
358

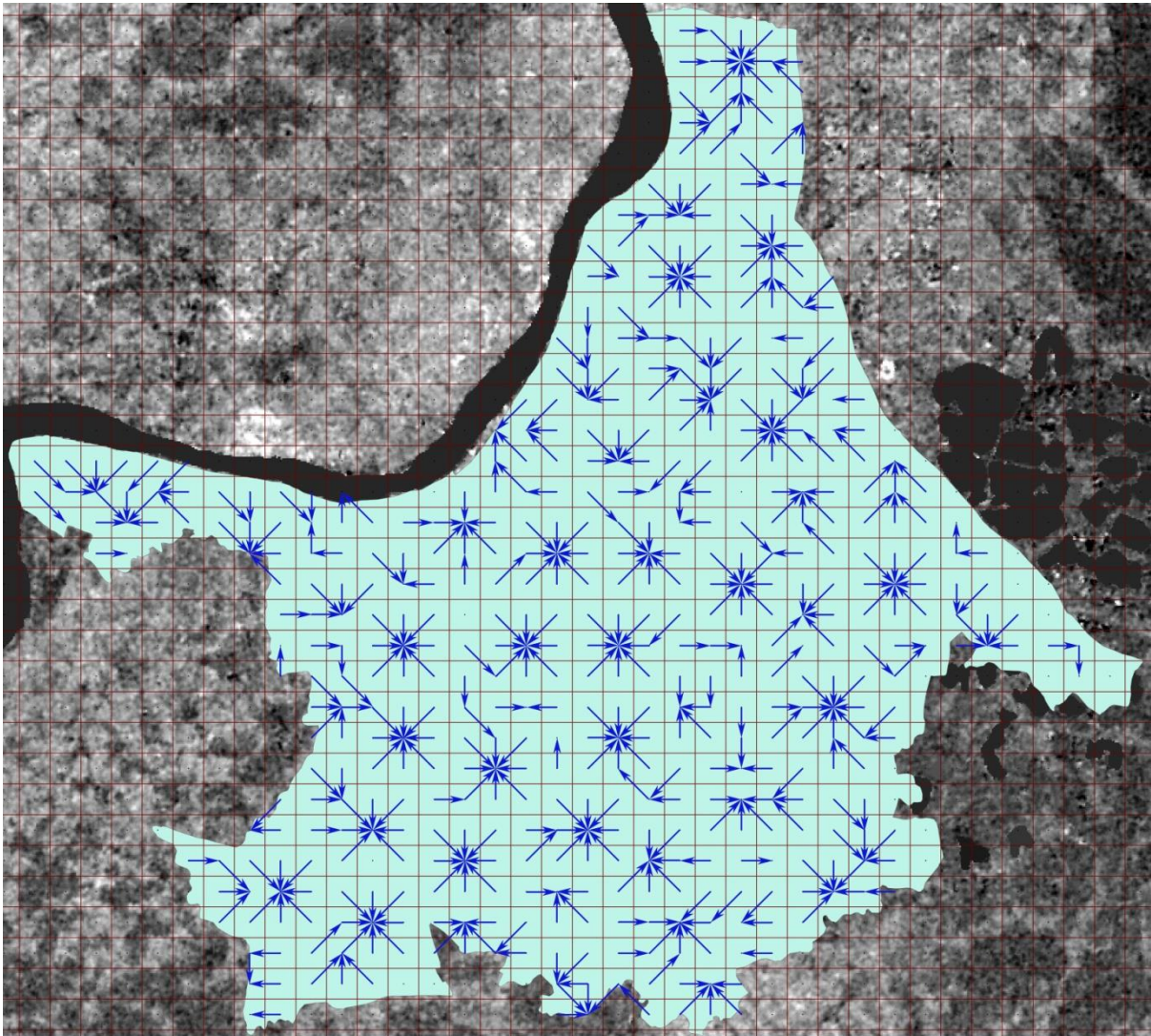
359 Next, we have used the **FD2O method** for the estimation of run-off. The
360 details of the calculation are already illustrated above. Here the value of Δx and Δy is
361 600 meters. Using the formula indicated in equations 2-5, $(\delta z/\delta x)_{i,j,k}$ and $(\delta z/\delta y)_{i,j,k}$ are
362 calculated. Using the values of $(\delta z/\delta x)_{i,j,k}$, and $(\delta z/\delta y)_{i,j,k}$, gradients are calculated using
363 the formula described in equation 6. The run-off pattern is calculated similarly to the
364 method described earlier and shown in (Fig. 11).
365



366
367 **Fig. 11.** Run-off pattern using **FD2O** method.
368

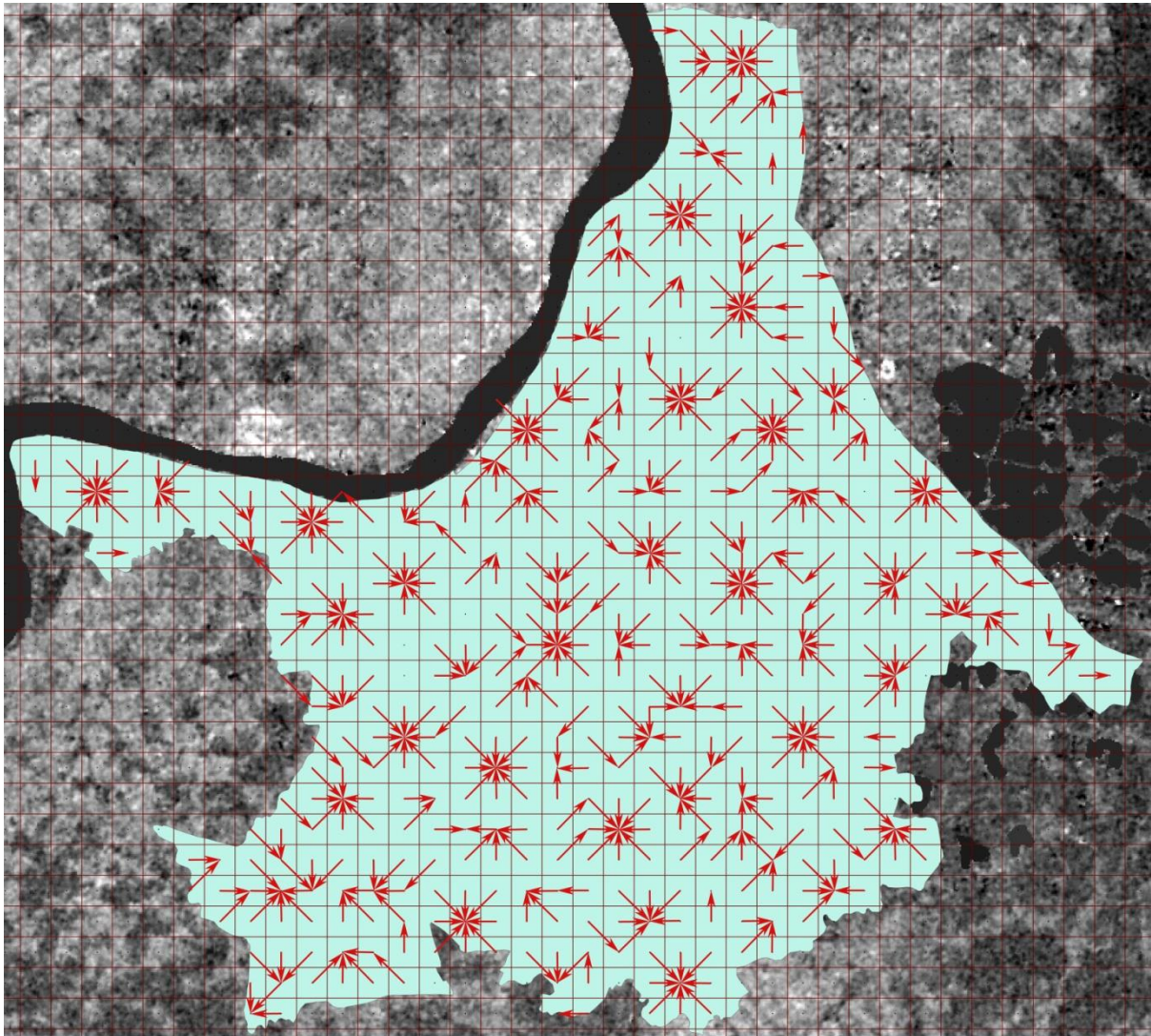
369
370
371
372
373
374
375
376
377

378 Next, we have used the third-order finite-difference technique to calculate $(\delta z/\delta x)_{i,j,k}$ and
379 $(\delta z/\delta y)_{i,j,k}$ gradients of various points. The $(\delta z/\delta x)_{i,j,k}$ and $(\delta z/\delta y)_{i,j,k}$ values are calculated to
380 estimate the gradient points. After determining the gradient points, a run-off pattern is also
381 calculated and shown in the next figure (Fig. 12).
382



383
384 **Fig. 12.** Run-off pattern using **FD3O** method.
385
386
387
388
389
390
391
392
393
394
395

396 Next, we have introduced a new method which is the fourth-order finite-difference technique
397 using which gradient is calculated. Skidmore (1989) used **D8A**, **FD20**, **FD30** methods
398 (partially) while calculating the gradient and aspect but never used the fourth-order finite-
399 difference method (**FD40**). In this method, $(\delta z/\delta x)_{i,j,k}$ and $(\delta z/\delta y)_{i,j,k}$ are calculated using the
400 fourth-order finite-difference technique using equations 7-10. Using the values of $(\delta z/\delta x)_{i,j,k}$
401 and $(\delta z/\delta y)_{i,j,k}$, the gradient is calculated using the formula described in equation 6. The run-
402 off pattern is next determined and shown in the next picture (Fig. 13).
403



404
405 **Fig. 13.** Run-off pattern using **FD40** method.
406

407 **5. Results Analysis**

408 **5.1. Waterlogging areas in Kolkata**

409 Before going to analysis of the flow pattern obtained using all four methods, the actual
410 scenario of the waterlogging areas of Kolkata is depicted below in Fig. 14. Kolkata is
411 infamous for the waterlogging problem. A large part of the city's low areas is deluged for a
412 considerable period disturbing city life to a large extent. It can be seen from the water logging
413
414

415 map of Kolkata that most waterlogging areas are as follows neglecting few water pockets
 416 scattered elsewhere.

-
- Maniktala
 - Sealdaha
 - Park Street
 - Ballygaunj
 - Bantala
 - Alipore
 - New Alipore
 - Jadavpur
 - Kudghat
 - Behala
-

417
 418 There are also some famous streets which are having a tendency to being waterlogged
 419 after a short rainfall. These are,

-
- Amherst Street
 - Lansdown Road.
 - CIT road
 - Part of BB gangly street
 - Part of MG road
 - Part of CR avenue
-

420

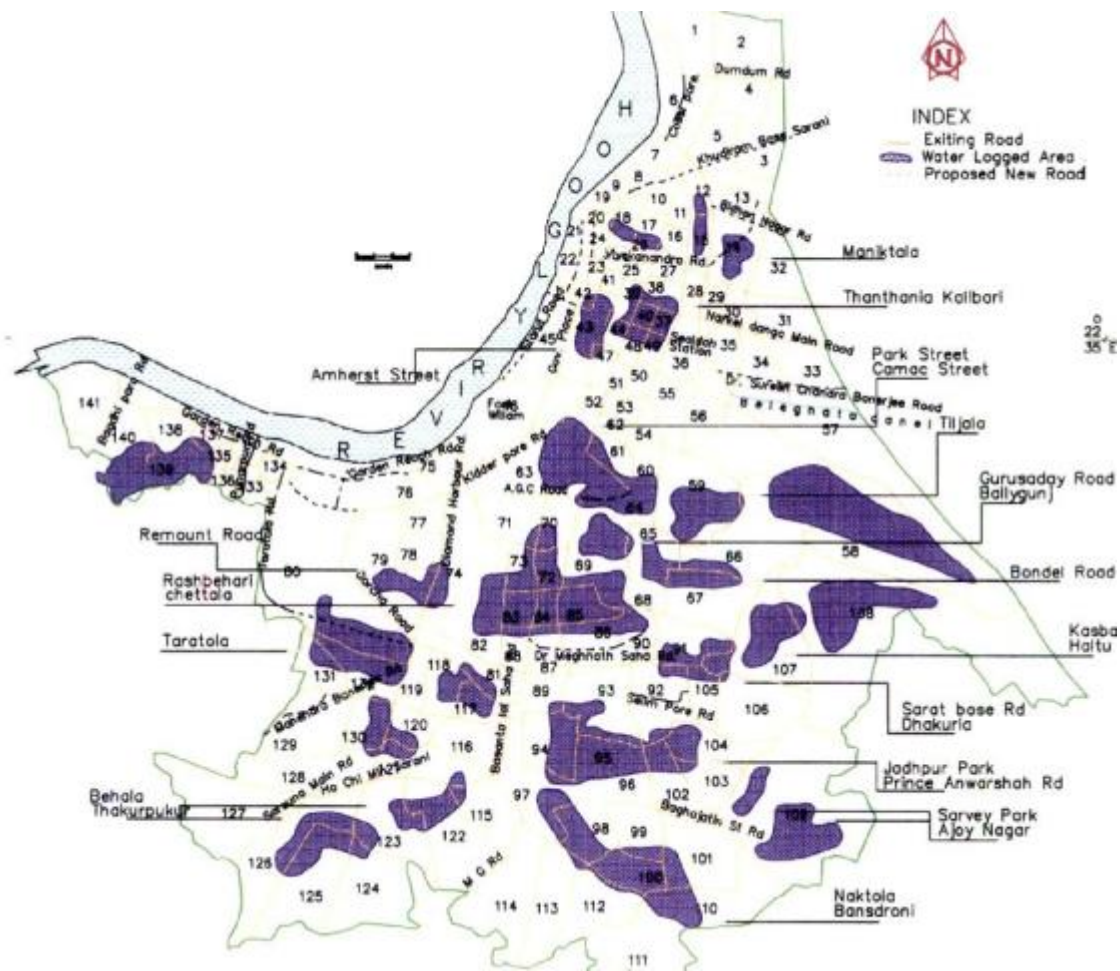


Fig. 14. Waterlogged map of Kolkata (Mukhopadhyay, 2004)

421

422

423

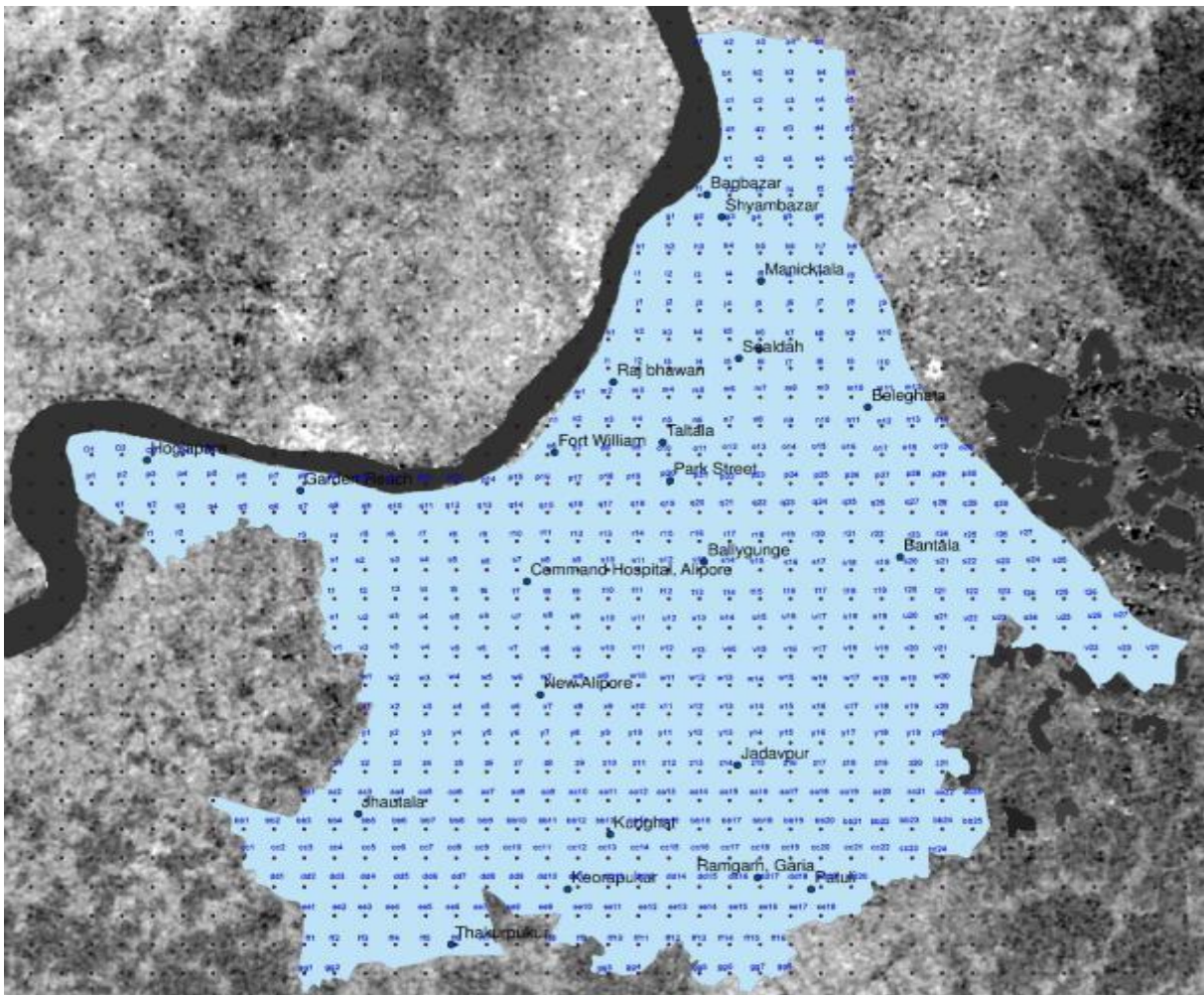
424 **5.2. Analysis**

425

426 The flow pattern from all these methods using 600 m × 600 m grids is further analyzed to
 427 determine the flow accumulation pattern in Kolkata. To find out the same, the following
 428 principle is followed. First, all the points in the grid system are given proper nomenclature. In
 429 the next picture (Fig. 15) a, b, c...aa, bb, etc. are denoted as rows and 1, 2 3... are progressive
 430 numbers along each row for 600 m × 600 m grid (Fig. 15). Based on the flow direction as

431 shown in the above pictures (for 600 m × 600 m cases), the number of cells contributing to
 432 any cell is determined.

433



434

435 **Fig. 16.** DEM of Kolkata with the nomenclature.

436

437 As an example, in Fig.16(a) flow is coming from nearest all eight (8) cells, then
 438 relative flow accumulation potential is described as 8. If the next any cell to the nearest
 439 eight-cell is also contributed to the above particular cell, the same is also added in the
 440 overall tally while finding out water logging potential. In Fig.16 (b) flow from
 441 surrounding three (3) cells also are contributing the centre cell $z_{i,j,k}$. Thus relative flow
 442 accumulation potential of $z_{i,j,k}$ is defined as 11.

443



444 **Fig. 16.** Flow accumulation Potential of (a) location $z_{i,j,k}$ is 8 and (b) location $z_{i,j,k}$ is 11.

445

446 In Table 1, we have identified three types of waterlogging areas, mild, moderate and massive.
 447 These names are given according to our postulation that a particular centre cell will be called
 448 a waterlogging area depending on how many surrounding cells water enter it. If the number
 449 of surrounding cells, from which water is coming towards the centre cell, increases then it
 450 implies that the centre cell area is more waterlogged. Here we look only at the massive
 451 waterlogged pockets of the study area. Accordingly using all the methods, we have estimated
 452 the most waterlogged areas and compared the results with the actual scenario. The flow
 453 accumulation potential for all points are thus determined using the above considerations.

454

455 **Table 1** Waterlogging potential postulation

Type of waterlogging area	Postulation
Mild	If the water is coming towards a centre cell from only 1-2 numbers of the surrounding cells
Moderate	If the water is coming towards a centre cell from 3-5 numbers of the surrounding cells
Massive	If the water is coming towards a centre cell from the 6-8 numbers of surrounding cells or more

456

457 After determining flow accumulation potential using all the above methods, we have
 458 compared the same with the potential waterlogging area of Kolkata. The main intention is to
 459 find out whether the outcome of these methods is matching with the outcome of all methods
 460 or not and which method is more accurate. More flow accumulation zones are identified
 461 considering run-off is coming from six (6) or more cells. Our assumption in this regard is that
 462 it is independent of any rainfall. It is also not taking any account of the simultaneous
 463 underground drainage pumping system effect. The flow accumulation areas as obtained from
 464 all four methods are shown in Figs. 17-20 and circled in red. Here all the areas like
 465 Maniktala, Sealdaha, Alipore, etc are demarcated as points. These points are randomly
 466 chosen within the given area.

467

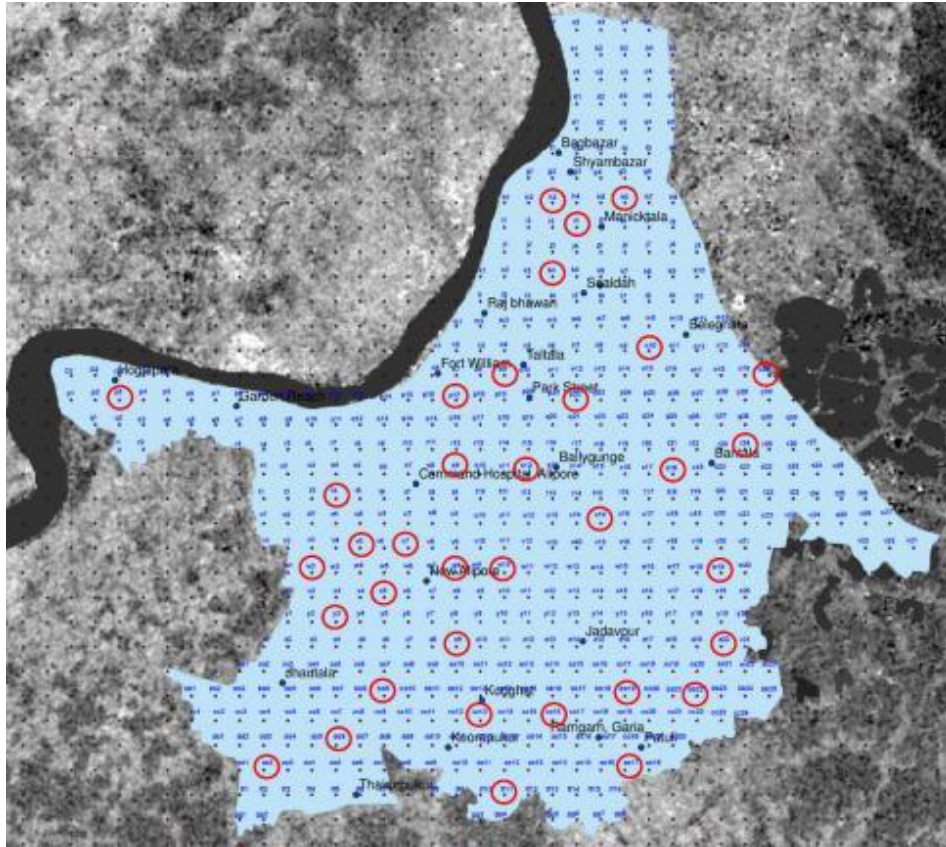


Fig. 17. Most waterlogged areas identified using the **D8A** method.

468
469
470

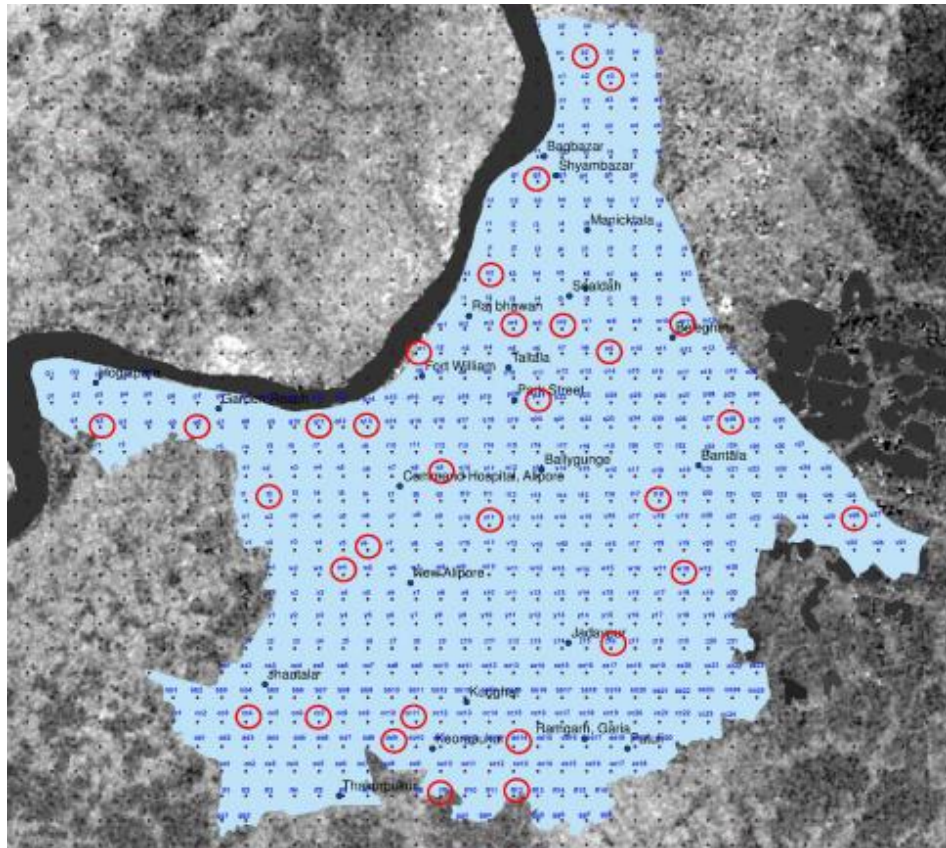


Fig. 18. Most waterlogged areas identified using the **FD20** method.

471
472

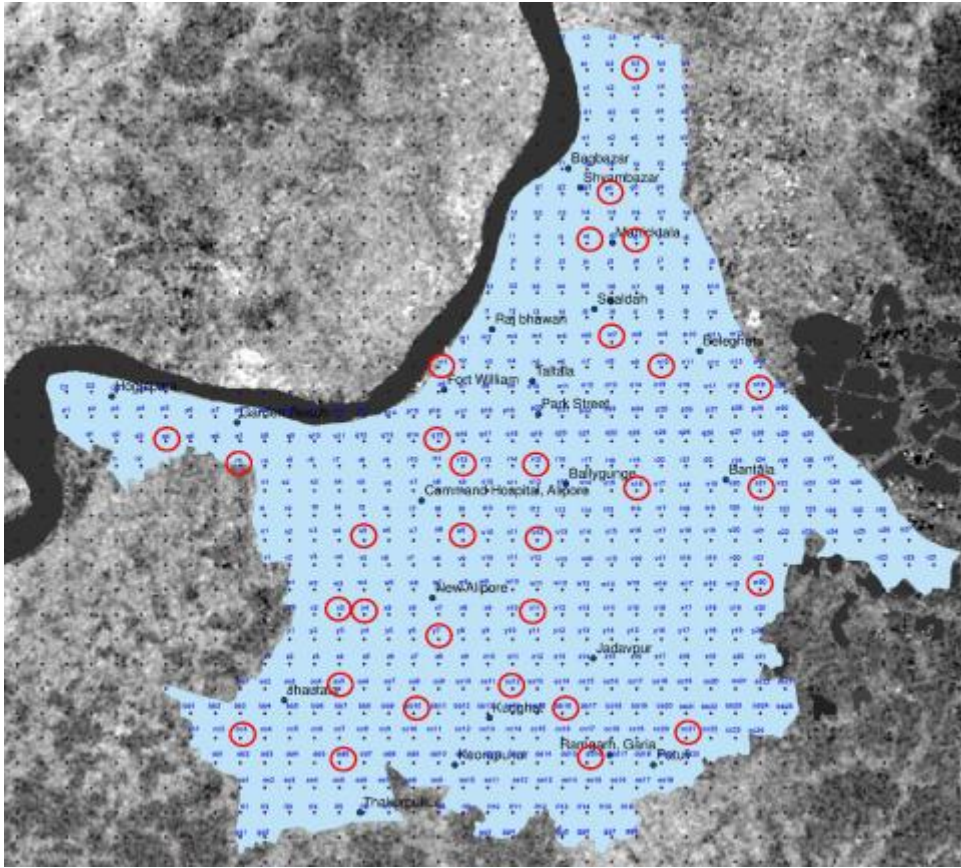


Fig. 19. Most waterlogged areas identified using the FD30 method.

473
474
475

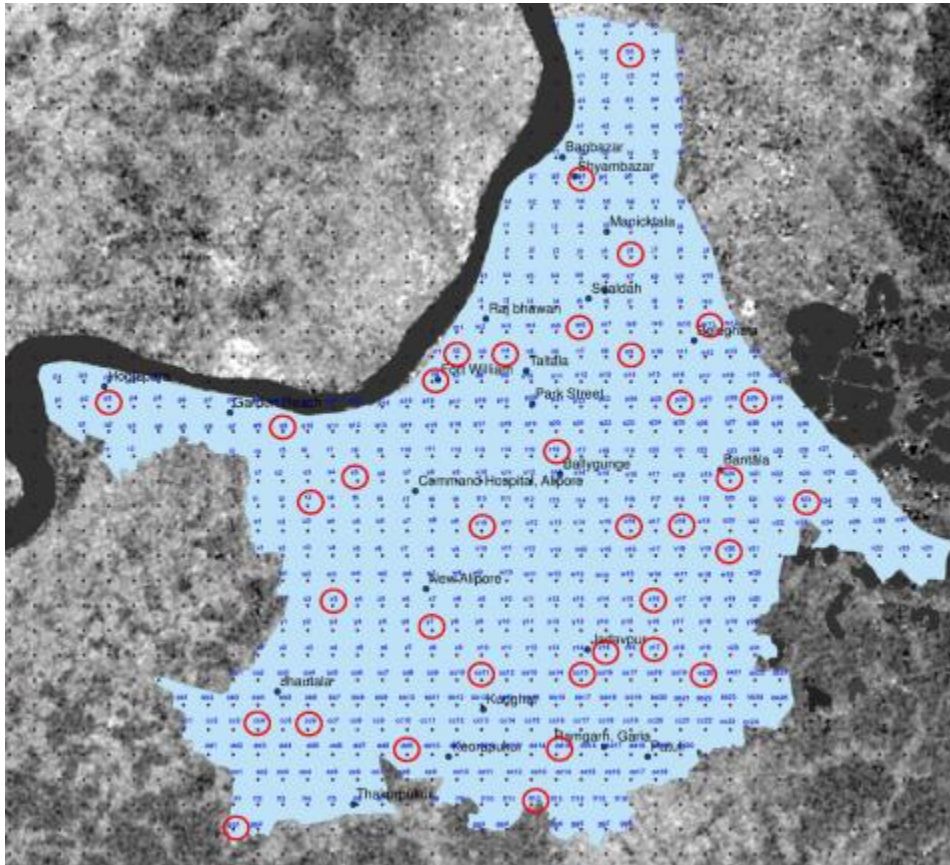


Fig. 20. Most waterlogged areas identified using the FD40 method.

476
477

478
 479
 480
 481
 482
 483
 484
 485
 486
 487
 488

Next, the flow accumulation area as evaluated from the above methods is compared with the above water logging map of Kolkata and the following inferences are deduced. It is actually compared whether the flow accumulation area of the left-hand side of Table 2 are matching with the map of Kolkata or not. If it is not matching then approximately, how far it deviates from the actual scenario is also deduced. Nevertheless, if we have considered that run-off is coming from five adjacent cells or less, then the number of waterlogging zones would have increased. Since we are about to find out the most waterlogging area, we are neglecting the potentially smaller waterlogging area.

Table 2 Waterlogging zone of Kolkata: A comparison of all methods

Area	D8A Method	FD20 Method	FD30 Method	FD40 Method
Maniktala	Matching	The nearest waterlogging area is 1.2 km (= 2 Δx) away	Matching	Matching
Sealdaha	The nearest waterlogging area is 0.6 km (= Δx) away	The nearest waterlogging area is 0.6 km (= Δx) away	The nearest waterlogging area is 0.6 km (= Δx) away	The nearest waterlogging area is 0.6 km (= Δx) away
Park Street	Matching	Matching	The nearest waterlogging area is 1.2 km (= 2 Δx) away	The nearest waterlogging area is 1.2 km (=2 Δx) away
Ballygaunj	Matching	The nearest waterlogging area is 1.2 km (= 2 Δx) away	The nearest waterlogging area is 0.6 km (= Δx) away	Matching
Bantala	The nearest waterlogging area is 0.6 km (= Δx) away	The nearest waterlogging area is 0.6 km (= Δx) away	Matching	Matching
Alipore	The nearest waterlogging area is 1.2 km (= 2 Δx) away	The nearest waterlogging area is 0.6 km (= Δx) away	The nearest waterlogging area is 0.6 km (= Δx) away	The nearest waterlogging area is 1.2 km (=2 Δx) away
New Alipore	Matching	The nearest waterlogging area is 1.2 km (= 2 Δx) away	The nearest waterlogging area is 0.6 km (= Δx) away	The nearest waterlogging area is 0.6 km (= Δx) away
Jadavpur	The nearest waterlogging area is 1.2 km (= 2 Δx) away	The nearest waterlogging area is 0.6 km (= Δx) away	The nearest waterlogging area is 1.2 km (= 2 Δx) away	Matching
Kudghat	Matching	The nearest waterlogging area is 1.2 km (=2 Δx) away	Matching	Matching
Behala	Matching	The nearest waterlogging area is 1.2 km (= 2 Δx) away	Matching	Matching

489
 490
 491

From the above Table 2, it can be identified that the D8A and FD40 methods are found to be more accurate amongst all methods.

492
493
494
495
496
497
498
499
500
501
502
503
504
505
506
507
508

5.3. Comparison of gradient values

The accuracy of the above methods can also be evaluated by the gradient of the respective points. Random points can be chosen over the DEM for the calculation of gradient points. However, for ease of identification, we have chosen the zones as mentioned in Table 2. The gradient can be calculated by all methods using equation 6 whereas the true gradient value can be calculated from the contour map. The calculated gradient of the selected zones already calculated using the above methods is indicated in Table 3. True gradient magnitudes are determined by hand by depicting a tangent on a contour-line going through the grid point and drawing a perpendicular tangent bisector. The gradient magnitude is computed by dividing the height difference with the perpendicular bisector by the perpendicular bisector length. It is by hand computed and values, as obtained from this method, are taken as the true values. Wherever the contour is not passing through the respective point(s), necessary interpolation is done between two adjacent contour curves. The contour map of Kolkata is indicated below in Fig. 21.

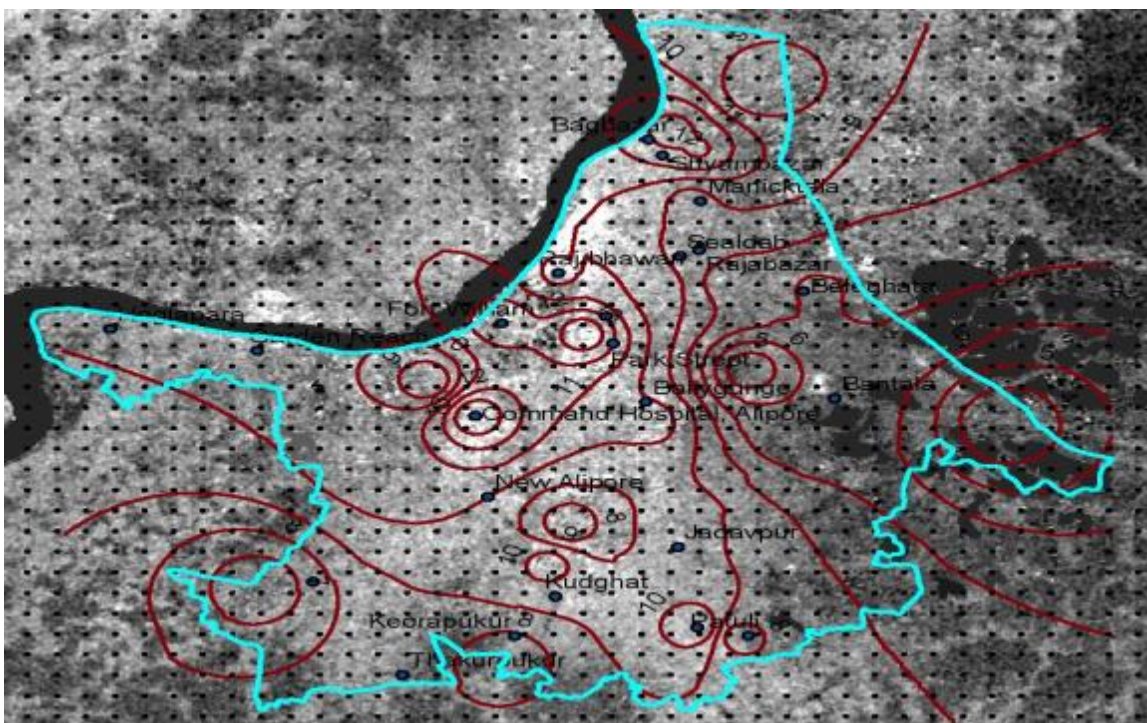


Fig. 21. Ground surface elevation contour map of Kolkata.

509
510
511
512
513
514
515
516
517
518
519

The gradient of all the points then calculated using equation 6 as described before and the ratio to the calculated gradient (C_g) and mean gradient values (C_{gm}) are calculated (Table 3).

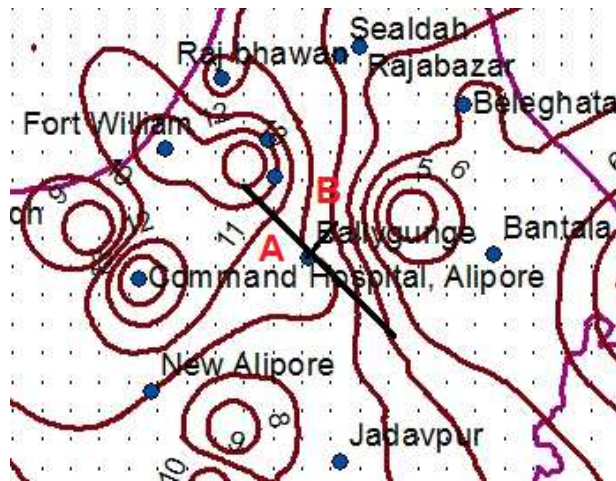
520 **Table 3** Gradient of selected points using all methods.

Sl. No. (n)	Area / Location	C_g/C_{gm} (D8 Model)	C_g/C_{gm} (Second Order)	C_g/C_{gm} (Third Order)	C_g/C_{gm} (Fourth Order)
1	Alipore	0.95	2.39	2.34	1.16
2	Ballygaunj	-0.49	1.15	0.60	1.76
3	Bantala	0.95	1.32	1.30	0.79
4	Behala	1.66	0.56	1.18	0.17
5	Jadavpur	0.49	0.00	0.22	0.30
6	Kudghat	0.72	0.56	0.58	0.59
7	Maniktala	0.95	0.74	0.58	0.87
8	New Alipore	1.43	0.41	0.58	0.97
9	Park Street	2.87	1.89	2.17	2.90
10	Sealdaha	0.49	0.98	0.46	0.50

521

522 Next, true gradient points are found out, which is the ratio to the difference between the
 523 elevation of adjacent two contour lines (sloping downwards) and the difference in distance
 524 between the points while calculated by drawing a bisector from the respective points as
 525 described above. A sample calculation (based on Fig. 22) is shown below using equation 15.

526



527 **Fig. 22.** Sample calculation of true gradient.

528

529

530 Let us assume that we have to measure the gradient value at point A (Ballygaunj). It is
 531 passing through the contour line having a value like 10. So first we need to draw a tangent
 532 along the contour line passing through point A. Thereafter perpendicular bisector needs to be
 533 drawn at point A. The same cuts the next lower contour line (with respect to point A) at point
 534 B. Point B is passing through contour line 9. Thus, the gradient of point A is as follows,

535

536 The Gradient at A =
$$\frac{\text{Difference between elevations at Point A and B}}{\text{The horizontal distance between A and B}} \quad (15)$$

537

538 Whenever any point is not passing through a contour line, necessary interpolation
 539 has been done to find out the elevation of this point.

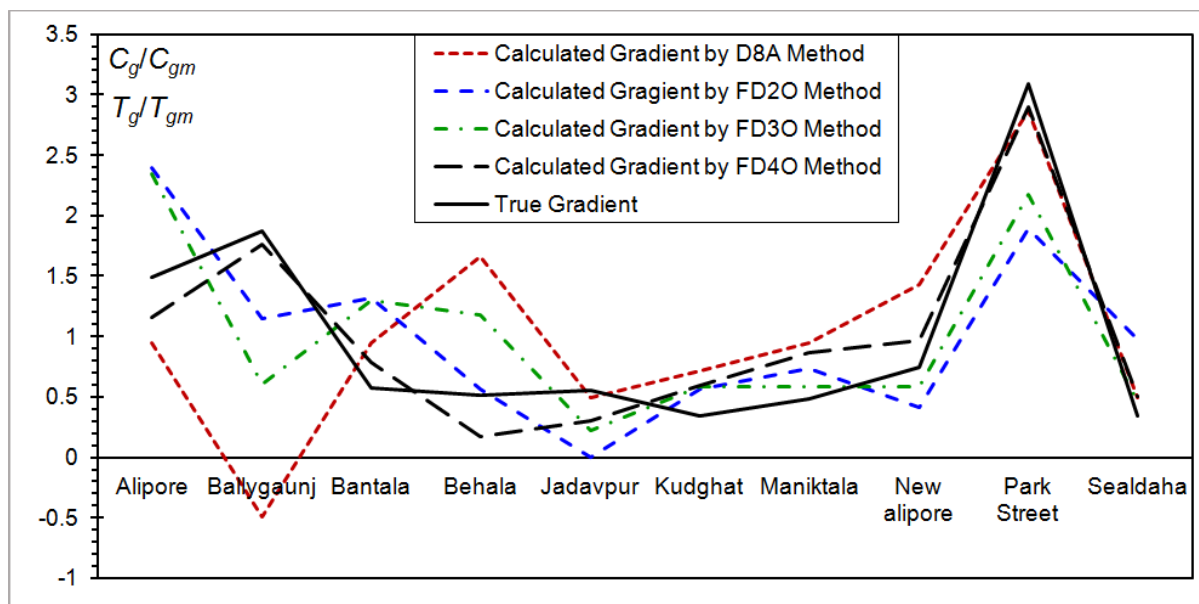
540

541 **5.4. Comparison of true and calculated gradients**

542

543 Values of true and calculated gradients as obtained based on the above are graphically
 544 compared and shown below in Fig. 23. The values of the true gradient (T_g) and calculated
 545 gradient (C_g) are normalized by their mean values T_{gm} and C_{gm} , respectively.

546



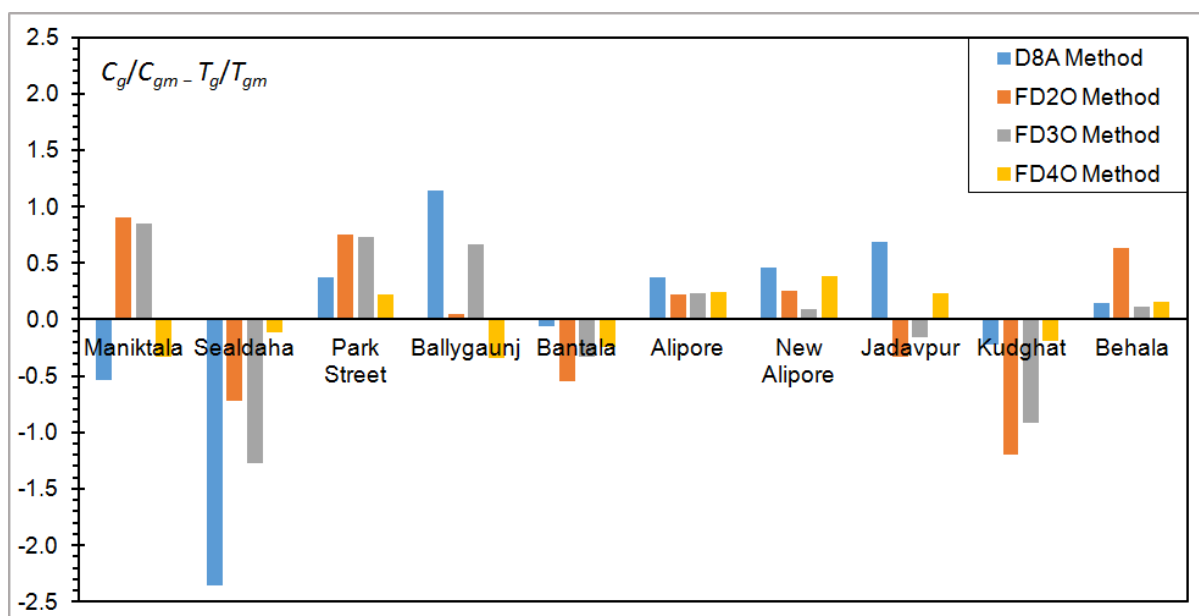
547

548 **Fig. 23.** Comparison of the normalized true and calculated gradients using the D8A, FD20,
 549 FD30, and FD40 methods.

550

551 It can be seen that there are some errors in the magnitude of 0.01 between true and calculated
 552 gradient. The same can be seen in the following bar chart (Fig. 24) for all the methods.

553



554

555 **Fig. 24.** The difference between normalized true and calculated gradients using the D8A,
 556 FD20, FD30, and FD40 methods.

557
558
559
560
561
562
563

The true gradient is calculated manually and a 600 m × 600 m grid is used. Hence error between these values is quite evident and cannot be ruled off. However, if we have considered in a particular zone using 100 m × 100 m cell or even smaller, the chances of error of these values can be further minimized.

564 **5.5. Spearman rank coefficient**

565
566
567
568
569
570
571
572

It is important to mention the monotonic function before describing Spearman’s correlation. A monotonic function is one that either never increases or never decreases as its independent variable increases. The monotonic function can be three types.

- 569 ○ Increasing monotonically: as the x variable increases the variable y never decreases.
- 570 ○ Decreasing monotonically: as the x variable increases the variable y never increases.
- 571 ○ Not monotonic: as the variable x increases the variable y sometimes decreases and
- 572 sometimes increases.

573
574
575

Spearman’s rank correlation coefficient is a statistical method to determine the strength of a monotonic relationship between paired data. It is denoted normally by r_{sp} . The value of r_{sp} normally falls as shown below in equation 17.

$$-1 \leq r_{sp} \leq +1 \tag{16}$$

577
578
579
580
581
582
583

The strength of the Spearman correlation between the calculated and true gradient values can be found out as follows,

- 579 ○ $0.00 \leq r_{sp} \leq 0.19$ implies - “very weak” correlation;
- 580 ○ $0.20 \leq r_{sp} \leq 0.39$ implies - “weak” correlation;
- 581 ○ $0.40 \leq r_{sp} \leq 0.59$ implies - “moderate” correlation;
- 582 ○ $0.60 \leq r_{sp} \leq 0.79$ implies - “strong” correlation;
- 583 ○ $0.80 \leq r_{sp} \leq 1.00$ implies - “very strong” correlation.

584

Spearman correlation coefficient can be defined as follows.

$$r_s = \frac{1-6 \sum d_i^2}{n(n^2-1)} \tag{17}$$

586

where n = number of points for the variable in question.

587
588

To find out the relation between the locations wise true and calculated gradients in each method, the Spearman correlation coefficient has been calculated.

589
590
591

Table 4 addresses the Spearman coefficient evaluation using the D8A method. Here, the Spearman coefficient r_s is found 0.369 and thereby the relationship between the true and calculated gradient is found weak.

592
593

Table 4 Spearman coefficient using the D8A method.

Location	C_g/C_{gm}	T_g/T_{gm}	x_i	y_i	$d_i= x_i-y_i$	d_i^2
Ballygaunj	-0.49	1.87	1	9	-8	64
Sealdaha	0.49	0.34	2	1	1	1
Jadavpur	0.49	0.55	3	5	-2	4

Kudghat	0.72	0.34	4	2	2	4
Maniktala	0.95	0.49	5	3	2	4
Bantala	0.95	0.57	6	6	0	0
Alipore	0.95	1.49	7	8	-1	1
New Alipore	1.43	0.74	8	7	1	1
Behala	1.66	0.51	9	4	5	25
Park Street	2.87	3.09	10	10	0	0

594

595 Table 5 illustrates the Spearman coefficient evaluation using the [FD2O method](#). Here, the
596 Spearman coefficient r_{sp} is found 0.612 and thereby the relationship between the true and
597 calculated gradient is found strong.

598

599 **Table 5** Spearman coefficient using the [FD2O method](#).

Location	C_g/C_{gm}	T_g/T_{gm}	x_i	y_i	$d_i = x_i - y_i$	d_i^2
Jadavpur	0.00	0.55	1	5	-4	16
New Alipore	0.41	0.74	2	7	-5	25
Kudghat	0.56	0.34	3	2	1	1
Behala	0.56	0.51	4	4	0	0
Maniktala	0.74	0.49	5	3	2	4
Sealdaha	0.98	0.34	6	1	5	25
Ballygaunj	1.15	1.87	9	9	0	0
Bantala	1.32	0.57	8	6	2	4
Park Street	1.89	3.09	9	10	-1	1
Alipore	2.39	1.49	10	8	2	4

600

601 Table 6 depicts the Spearman coefficient evaluation using the [FD3O method](#). In this method,
602 the Spearman coefficient r_{sp} is found 0.624 and thereby the relationship between the true and
603 calculated gradient is found strong.

604

605 **Table 6** Spearman coefficient evaluation using the [FD3O method](#).

Location	C_g/C_{gm}	T_g/T_{gm}	x_i	y_i	$d_i = x_i - y_i$	d_i^2
Jadavpur	0.22	0.55	1	5	-4	16
Sealdaha	0.46	0.34	2	1	1	1
Maniktala	0.58	0.49	3	3	0	0
New alipore	0.58	0.74	4	7	-3	9
Kudghat	0.58	0.34	5	2	3	9
Ballygaunj	0.60	1.87	6	9	-3	9
Behala	1.18	0.51	7	4	3	9
Bantala	1.30	0.57	8	6	2	4
Park Street	2.17	3.09	9	10	-1	1
Alipore	2.34	1.49	10	8	2	4

606

607 Table 7 highlights the Spearman coefficient evaluation using the FD4O method. Here, the
 608 Spearman coefficient r_{sp} is found 0.7818 and thereby the relationship between the true and
 609 calculated gradient is found nearly very strong.

610

611 **Table 7** Spearman coefficient evaluation using the FD4O method.

Location	C_g/C_{gm}	T_g/T_{gm}	x_i	y_i	$d_i = x_i - y_i$	d_i^2
Behala	0.17	0.51	1	4	-3	9
Jadavpur	0.30	0.55	2	5	-3	9
Sealdaha	0.50	0.34	3	1	2	4
Kudghat	0.59	0.34	4	2	2	4
Bantala	0.79	0.57	5	6	-1	1
Maniktala	0.87	0.49	6	3	3	9
New Alipore	0.97	0.74	7	7	0	0
Alipore	1.16	1.49	8	8	0	0
Ballygaunj	1.76	1.87	9	9	0	0
Park Street	2.90	3.09	10	10	0	0

612

613 Therefore, from Tables 4-7, it is clear that the FD4O method is the most accurate amongst all
 614 the methods considered here.

615 The next statistical analysis is carried out to establish the fact of whether the FD4O
 616 method is more accurate or not. Here we have used root-mean-square-error (RMSE),
 617 relative root-mean-square-error (RRMSE), G test, and mean difference method between
 618 true and calculated gradient values.

$$619 \quad \text{RMSE} = \sqrt{\frac{\sum_{i=1}^n (C_{gi} - T_{gi})^2}{n-1}} \quad (18)$$

$$620 \quad \text{RRMSE} = \frac{1}{n} \sum_{i=1}^n \frac{C_{gi} - T_{gi}}{T_{gi}} \quad (19)$$

$$621 \quad \text{Mean Difference} = \frac{1}{n} \sum_{i=1}^n (C_{gi} - T_{gi}) \quad (20)$$

$$622 \quad G = \frac{1}{n} 2 \sum_{n=1}^{10} C_{gi} \ln \frac{C_{gi}}{T_{gi}} \quad \text{iff} \quad C_{gi} \geq 0 \quad (21)$$

623

624 Based on the above equations 18-21, RMSE, RRMSE, G test and mean differences are
 625 calculated and indicated in Table 8.

626 The RMSE value was found minimum for the FD4O method. The RRMSE and mean
 627 difference values are lowest for the D8A and FD4O methods, respectively. Hence it can be
 628 furnished that the error in D8A and FD4O methods is less and the calculated gradient value
 629 has a tendency to coincide with the true gradient value.

630

631 **Table 8** RMSE, RRMSE, G test, Mean difference values of all methods

Method	RMSE	RRMSE	Mean difference	G Test
D8A	0.003139	0.73	0.000577	0.00410
FD2O	0.003105	1.06	0.001697	0.00622
FD3O	0.002734	0.79	0.001237	0.00440
FD4O	0.001619	0.55	0.001127	0.00309

632

633 The RRMSE is more sensitive for estimating gradient errors for plain locations, as large
 634 estimated gradient errors in shallow slopes will provide a greater effect on indicator value
 635 than equivalent gradient errors for areas with steeper slopes (Warren et al., 2004). Here the
 636 least RRMSE is observed when [applying the FD4O method](#). It agrees with the observation of
 637 Warren et al. (2004) and confirms that the [FD4O method](#) is the best in estimating the gradient
 638 and slopes of plain areas. From the observed RMSE and G test values, it is not possible to
 639 correlate which method is superior. According to the 95% Confidence intervals test, the [D8A](#)
 640 [and FD4O methods](#) have considerably lower gradient estimation errors than the [FD2O and](#)
 641 [FD3O methods](#).

642 For determining the water logging potential in a smaller area, the grid can be considered
 643 100 m × 100 m or even less so that the chances of any error can be further reduced. Also for a
 644 bigger plain surface like Kolkata, a better result could be obtained if we can focus on any
 645 particular area and then study the water logging spots road wise and validate the same from
 646 actual data. The waterlogging area of the deltaic city Kolkata depends on its various drainage
 647 conditions like details of the drainage pumping station, condition and size of drainage pipe
 648 and channel, contribution of drainage flow from the surrounding area, etc. These other
 649 conditions reduced some percentage of accuracy of all the four methods applied herein.
 650 However, these methods can be applied to rural plain regions having an area of 200 sq km
 651 wherein a proper drainage system not exists, and results can be analyzed with a high accuracy
 652 accordingly.

653 As a further scope of the study, using multi linear models using regression can be
 654 reviewed for estimation of the gradient of a plain surface. Also for a large plain surface area
 655 (area in the tune of 500 sq. km), it is possible to check whether a sufficient accuracy level can
 656 be obtained from the [D8A method or FD4O method](#) or not using 600 m × 600 m grid. For
 657 calculation of the gradient point, it is seen that as the grid shortens, calculated gradient value
 658 approaches towards true gradient value irrespective of any methods. This deduction can be
 659 further cross-checked for a smaller zone and the strength of the Spearman coefficient
 660 between these two variables can be checked. An alternative Kendall tau coefficient can be
 661 obtained to check the relationship of these variables as was also done on a hilly surface by
 662 Skidmore (1989).

663

664 **6. Conclusions**

665

666 It can be concluded that the [D8A method \(D8 algorithm\)](#) and the [FD4O method](#) (finite
 667 difference technique of fourth order) are mostly correct with comparison to other methods
 668 like the [FD2O method](#) (finite difference technique of second order) and [FD3O method](#) (finite

669 difference technique of third order) while determining the flow accumulation potential of
670 a plain surface. The flow accumulation zones of a plain surface region, here deltaic city
671 Kolkata, as derived from the [D8A method](#) and the [FD4O method](#) are matching the actual
672 flow accumulation area and waterlogging area of Kolkata. Hence, we can therefore
673 conclude that the [D8A method and FD4O methods](#) are best suitable while determining
674 water logging potential and flow pattern on a plain surface. Between [methods FD2O and](#)
675 [FD3O](#), [FD3O](#) happens to be more accurate than the [FD2O](#) method. For such comparative
676 analysis, the Spearman rank coefficient method is proven to be the most appropriate
677 compared to other statistical methods like RMSE, RRMSE, G test, and mean difference
678 method.

679 As the accuracy level is increased from second-order to fourth-order finite-
680 difference, the strength of the variables (i.e. true and calculated gradients) becomes
681 stronger and stronger. For a hilly forest region, there is hardly any difference in the value
682 of the Spearman coefficient between methods like [the D8A and FD3O methods](#). So as
683 the error in the finite difference model decreases, the strength of variables becomes more
684 and more prominent which also points to the fact that if we go for the fourth or higher-
685 order finite-difference model gradient can be more accurately calculated and more
686 prominently flow accumulation area or the waterlogging area of a plain surface can be
687 determined which is in line with our earlier deduction. Nevertheless, the accuracy level
688 will be further increased if we go for smaller size grids. In another way, the fourth order
689 finite-difference model can be used to get a reasonable accuracy to determine the flow
690 accumulation potential of plain surface (area in the tune of 200 sq km). However, if a
691 smaller plain surface area is chosen with a smaller grid size, the accuracy level will
692 definitely be increased. Similarly, for a large plain surface area (area in the tune of 500
693 sq km or more) fourth-order finite-difference ([FD4O](#)) method [or D8 algorithm \(D8A\)](#)
694 [method](#) with a higher accuracy level can be successfully used.

695

696 **Declarations**

697

698 The authors have no relevant financial or non-financial interests to disclose. The authors have
699 no conflicts of interest to declare that are relevant to the content of this article.

700

701 **References**

702

703 Anderson JDJ (1995) Computational Fluid Dynamics – The Basics with Applications.
704 International Editions, Schaum Division, McGraw-Hill Inc., New York

705 Ashraf MI, Zhao Z, Bourque CPA, Meng F (2011) GIS-evaluation of two slope-calculation
706 methods regarding their suitability in slope analysis using high-precision LiDAR
707 digital elevation models. *Hydrol Process* 26(8):1119–1133.
708 <https://doi.org/10.1002/hyp.8195>

709 Banerjee S (2018) An Analysis of Urban Flooding Scenario in the City of Kolkata, West
710 Bengal. *Int J Innov Knowl Concept* 6(5):1–9. <https://doi.org/11.25835/IJK-24>

711 Beasley DB, Huggins LF, Monke EJ (1980) A model for watershed planning. *Trans Am Soc*
712 *Agric Eng* 23(4):938–944. <https://doi.org/10.13031/2013.34692>

713 Beven KJ, Kirkby MJ (1979) A physically based, variable contributing area model of basin
714 hydrology. *Hydrol Sci Bull* 24(1):43–69. <https://doi.org/10.1080/02626667909491834>

715 Bolstad PV, Stowe T (1994) An Evaluation of DEM Accuracy: Elevation, Slope, and Aspect.
716 *Photogramm Eng Remote Sens* 60(11):1327–1332

717 Chavda DB, Makwana JJ, Parmar HV, Kunapara AN, Parajapati GV (2016) Estimation of
718 Runoff for Ozat Catchment using RS and GIS based SCS-CN method. *Curr World*
719 *Environ* 11(1):212–217. <http://dx.doi.org/10.12944/CWE.11.1.26>

720 Cabral MCC, Burges SJ (1994) Digital Elevation Model Networks (DEMON): A model of
721 flow over hillslopes for computation of contributing and dispersal areas. *Water*
722 *Resour Res* 30(6):1681–1692. <https://doi.org/10.1029/93WR03512>

723 Das S, Patel PP, Sengupta S (2016) Evaluation of different digital elevation models
724 for analyzing drainage morphometric parameters in a mountainous terrain: a case
725 study of the Supin–Upper Tons Basin, Indian Himalayas. *SpringerPlus* 5:1544.
726 <https://doi.org/10.1186/s40064-016-3207-0>

727 Dasgupta S, Roy S, Sarraf M (2012) Urban Flooding in a Changing Climate: Case Study of
728 Kolkata, India. *Asian-Afr J Econ Econometric* 12(1):135–158.

729 Fairfield J, Leymarie P (1991) Drainage networks from grid elevation models. *Water Resour*
730 *Res* 27(5):709–717. <https://doi.org/10.1029/90WR02658>

731 Fortin JP, Turcotte R, Massicotte S, Moussa R, Fitzback J, Villeneuve JP (2001) A
732 distributed watershed model compatible with remote sensing and GIS Data, I:
733 Description of model. *J Hydrol Eng* 6(2):91–99.
734 [https://doi.org/10.1061/\(ASCE\)1084-0699\(2001\)6:2\(91\)](https://doi.org/10.1061/(ASCE)1084-0699(2001)6:2(91))

735 Gayathri, C. & Jayalakshmi, S. (2018) Estimation of Surface Runoff Using Remote Sensing
736 and GIS Techniques for Cheyyar Sub Basin. *Int J Eng Res Tech* 6(7):1–5.

737 Graham A, Coops NC, Wilcox M, Plowright A (2018) Evaluation of Ground Surface Models
738 Derived from Unmanned Aerial Systems with Digital Aerial Photogrammetry in a
739 Disturbed Conifer Forest. *Remote Sens* 11(1):84. <https://doi.org/10.3390/rs11010084>

740 Grey V, Livesley SJ, Fletcher TD, Szota C (2018) Establishing street trees in stormwater
741 control measures can double tree growth when extended waterlogging is avoided.
742 *Landsc Urb Plan* 178:122–129. <https://doi.org/10.1016/j.landurbplan.2018.06.002>

743 Guo-an T, Strobl J, Gong J, Zhao M, Chen Z (2001) Evaluation on the accuracy of digital
744 elevation models. *J Geogr Sci* 11(2):209–216. <https://doi.org/10.1007/BF02888692>

745 John B, Das S (2020) Identification of risk zone area of declining piezometric level in the
746 urbanized regions around the City of Kolkata based on ground investigation and GIS
747 techniques. *Groundw Sustain Dev* 11:100354.
748 <https://doi.org/10.1016/j.gsd.2020.100354>

749 John B, Das S, Das R (2020) Effect of changing land use scenario in Kolkata Metropolitan on
750 the variation in volume of runoff using multi-temporal satellite images. *J Indian Chem*
751 *Soc* 97(4):555–562

752 Kok K, Sidek LM, Jung K, Kim J (2018) Analysis of Runoff Aggregation Structures with
753 Different Flow Direction Methods under the Framework of Power Law Distribution.
754 *Water Resour Manag* 32:4607–4623. <https://doi.org/10.1007/s11269-018-2074-6>

755 Kumar PS, Praveen TV, Prasad MA (2016) Rainfall-Runoff Modelling using Modified
756 NRCS-CN, RS and GIS -A Case Study. *Int J Eng Res Appl* 6(3):54–58

757 Martz LW, Garbrecht J (1992) Numerical definition of drainage network and subcatchment
758 areas from Digital Elevation Models. *Computer Geosci* 18(6):747–761.
759 [https://doi.org/10.1016/0098-3004\(92\)90007-E](https://doi.org/10.1016/0098-3004(92)90007-E)

760 Mukhopadhyay A (2004) Geomorphology of Kolkata municipal corporation KMC its impact
761 on urban functions. Ph.D. Thesis, Department of Geography, University of Calcutta,
762 India. <http://hdl.handle.net/10603/159507>

763 O’Callaghan J, Mark D (1984) The extraction of drainage networks from digital elevation
764 data. *Computer Vis Gr Imag Process* 28(3):323–344. [https://doi.org/10.1016/S0734-189X\(84\)80011-0](https://doi.org/10.1016/S0734-189X(84)80011-0)

766 Paul A (2009) Assessment of waterlogging in C M C and its social impact. Ph.D. Thesis,
767 Department of Geography, University of Calcutta, India.
768 <http://hdl.handle.net/10603/154829>

769 Pike AS (2006) Application of digital terrain analysis to estimate hydrological variables in
770 the Luquillo Mountains of Puerto Rico. *Climate Variability and Change—*
771 *Hydrological Impacts (Proceedings of the Fifth FRIEND World Conference held at*
772 *Havana, Cuba, November 2006)*, pp. 81–86

773 Quinn P, Beven KJ, Chevalier P, Planchon O (1991) The prediction of hillslope flow paths
774 for distributed hydrological modelling using digital terrain models. *Hydrol Process*
775 5(1):59-79. <https://doi.org/10.1002/hyp.3360050106>

776 Rana VK, Suryanarayana TMV (2020) GIS-based multi criteria decision making method to
777 identify potential runoff storage zones within watershed. *Ann GIS* 26(2):149-168.
778 <https://doi.org/10.1080/19475683.2020.1733083>

779 Rhind DW (2013) Automated Contouring-an Empirical Evaluation of Some Differing
780 Techniques. *Cartogr J* 8(2):145–158. <https://doi.org/10.1179/00087041.8.2.p145>

781 Roy R, Dhali MK (2016) Seasonal Water logging Problem In A Mega City: A Study of
782 Kolkata, India. *J Res Humanit Soc Sci* 4(4):01–09

783 Sar N, Chatterjee S, Adhikari MD (2015) Integrated remote sensing and GIS based spatial
784 modelling through analytical hierarchy process (AHP) for water logging hazard,
785 vulnerability and risk assessment in Keleghai river basin, India. *Model Earth Syst*
786 *Environ* 1: 31. <https://doi.org/10.1007/s40808-015-0039-9>

787 Satheeshkumar S, Venkateswaran S, Kannan R (2017) Rainfall–runoff estimation using
788 SCS–CN and GIS approach in the Pappiredipatti watershed of the Vaniyar sub basin,
789 South India. *Model Earth Syst Environ* 3:24. <https://doi.org/10.1007/s40808-017-0301-4>

791 Skidmore AK (1989) A comparison of techniques for calculating gradient and aspect from a
792 gridded digital elevation model. *Int J Geogr Inf Syst* 3(4):323–334.
793 <https://doi.org/10.1080/02693798908941519>

794 Solomon H (2005) GIS based Surface Run-off modelling and Analysis of contributing
795 factors: A Case Study of Nam Chun Watershed, Thailand. International Institute for
796 Geo-Information science and earth observation Enschede, The Netherlands, pp. 1–110

797 Stuebe MM, Johnston DM (1990) Runoff Volume estimation using GIS techniques. *J Am*
798 *Water Resour Assoc* 26(4):611–620. <https://doi.org/10.1111/j.1752->
799 [1688.1990.tb01398.x](https://doi.org/10.1111/j.1752-1688.1990.tb01398.x)

800 Su B, Huang H, Li Y (2015) Integrated simulation method for waterlogging and traffic
801 congestion under urban rainstorms. *Nat Hazard* 81:23–40.
802 <https://doi.org/10.1007/s11069-015-2064-4>

803 Tarboton DG (1997) A new method for the determination of flow directions and upslope
804 areas in grid digital elevation models. *Water Resour Res* 33(2):309–319.
805 <https://doi.org/10.1029/96WR03137>

806 Tran D, Xu D, Dang V, Alwah AAQ (2020) Predicting Urban Waterlogging Risks by
807 Regression Models and Internet Open-Data Sources. *Water* 12(3):879.
808 <https://doi.org/10.3390/w12030879>

809 Vizzari M, Hilal M, Sigura M, Antognelli S, Joly D (2018) Urban-rural-natural gradient
810 analysis with CORINE data: An application to the metropolitan France. *Landsc Urb*
811 *Plan* 171:18-29. <https://doi.org/10.1016/j.landurbplan.2017.11.005>

812 Vojtek M, Vojteková J (2016) GIS-based Approach to Estimate Surface Runoff in Small
813 Catchments: A Case Study. *Quaest Geogr* 35(3):1–20.
814 <https://doi.org/10.1515/quageo-2016-0030>

815 Warren SD, Hohmann MG, Auerswald K, Mitasova H (2004) An evaluation of methods to
816 determine slope using digital elevation data. *Catena* 58:215–233.
817 <https://doi.org/10.1016/j.catena.2004.05.001>

818 Xue F, Huang M, Wang W, Zou L (2016) Numerical simulation of Urban Waterlogging
819 Based on Flood Area Model. *Adv Meteorol* 3940707.
820 <https://doi.org/10.1155/2016/3940707>

821 Zhao G, Gao J, Tian P, Tian K (2009) Comparison of two different methods for determining
822 flow direction in catchment hydrological modelling. *Water Sci Eng* 2(4):1–15.
823 <https://doi.org/10.3882/j.issn.1674-2370.2009.04.001>

824 Zhou Q, Pilesjö P, Chen Y (2010) Estimating surface flow paths on a digital elevation model
825 using a triangular facet network. *Water Resour Res* 47(7):1–12.
826 <https://doi.org/10.1029/2010WR009961>